Constraints on the CKM Unitarity Triangle from Charmless 3-body Decays at BABAR

Thomas Latham

THE UNIVERSITY OF WARWICK

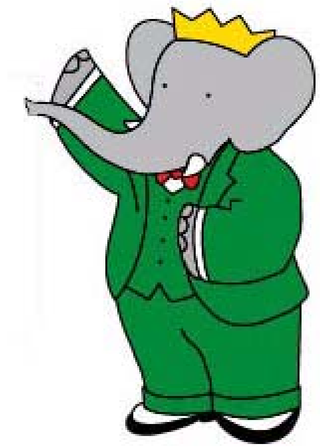

Overview

- Introduction
  - Detector & Dataset
  - CP violation
  - Analysis Techniques
  - Theory Motivation
- Recent results from BaBar:
  - $B^+ \to K^+\pi^+\pi^-$
  - $B^0 \to K_S\pi^+\pi^-$
  - $B^0 \to K^+\pi^-\pi^0$
- Conclusion

PEP II and BaBar

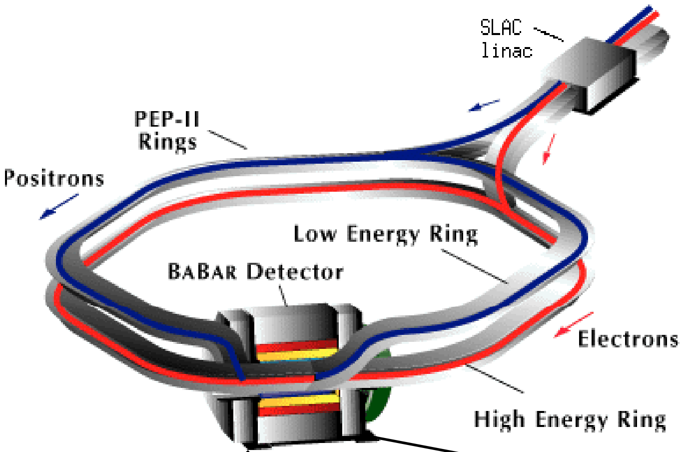

- PEP II/BaBar *B*-Factory located at Stanford Linear Accelerator Center
- Collided beams of electrons and positrons with asymmetric energies

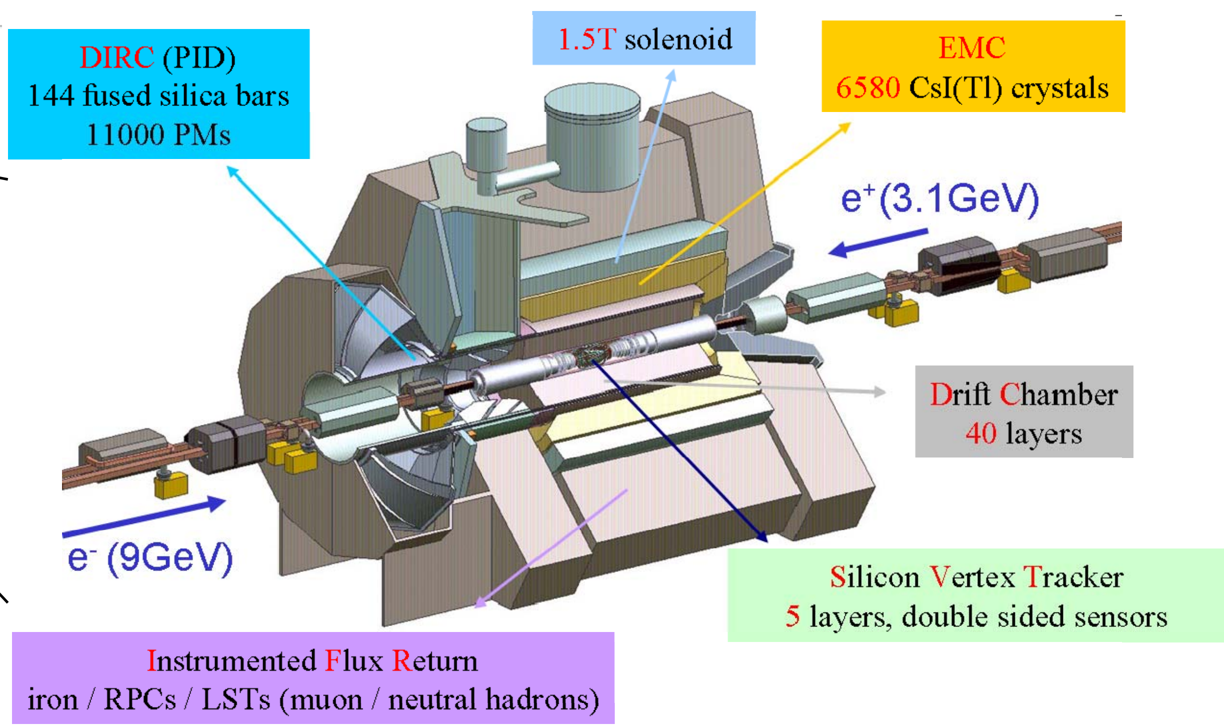

Dataset

- BaBar data-taking ended on 7th April 2008
- Total of ~531 fb^{-1} recorded, ~432 fb^{-1} at the Υ(4S)
- Analyses presented here use either 232 or 383 million BB pairs

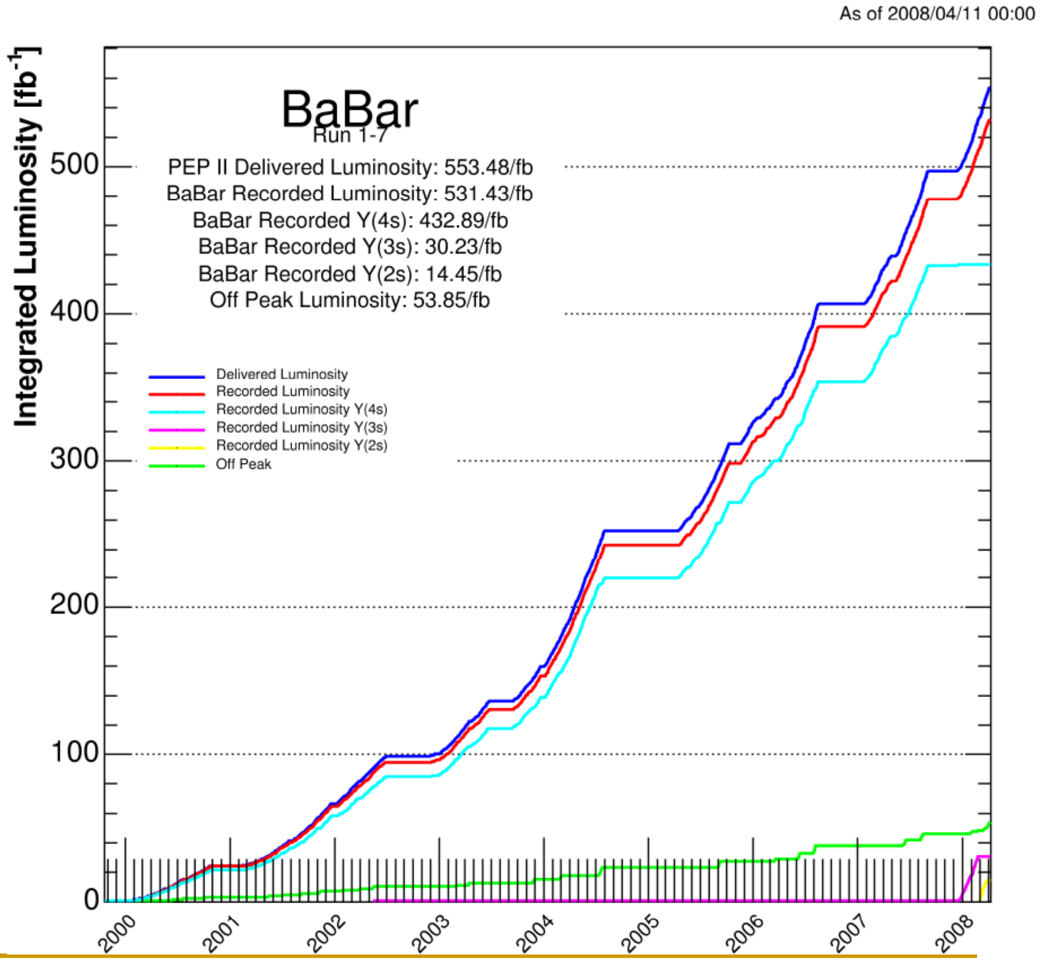

The CKM Mechanism

- *CP* violation in the Standard Model arises from a single phase in the quark-mixing (CKM) matrix

$$\begin{pmatrix} d' \\ s' \\ b' \end{pmatrix} = \begin{pmatrix} V_{ud} & V_{us} & V_{ub} \\ V_{cd} & V_{cs} & V_{cb} \\ V_{td} & V_{ts} & V_{tb} \end{pmatrix} \begin{pmatrix} d \\ s \\ b \end{pmatrix}$$

$$V_{\mathrm{CKM}} \approx \begin{pmatrix} 1-\frac{\lambda^2}{2} & \lambda & A\lambda^3(\rho - i\eta) \\ -\lambda & 1-\frac{\lambda^2}{2} & A\lambda^2 \\ A\lambda^3(1-\rho-i\eta) & -A\lambda^2 & 1 \end{pmatrix} + \mathcal{O}(\lambda^4)$$

- Unitarity conditions of matrix can be expressed as triangles in complex plane

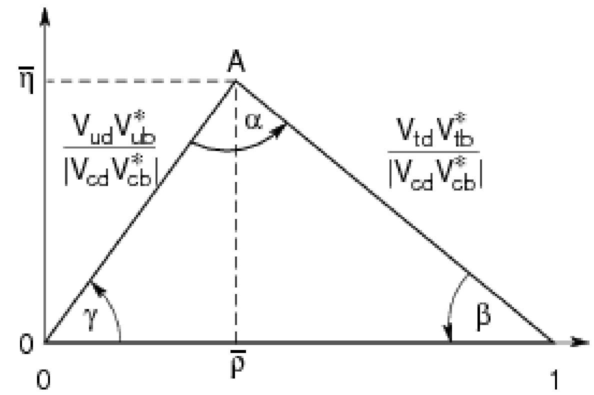

$$V_{ud}V_{ub}^* + V_{cd}V_{cb}^* + V_{td}V_{tb}^* = 0$$

- Half of 2008 Nobel Prize in physics awarded to Kobayashi and Maskawa

Direct *CP* Violation

- *CP* violation in decay
- $A \neq \bar{A}$ – both Figs. (a) & (b)
- Rate asymmetry requires two amplitudes with both different weak and strong phases to contribute – Fig. (b)
- Observed in decays of neutral *K* and *B* mesons

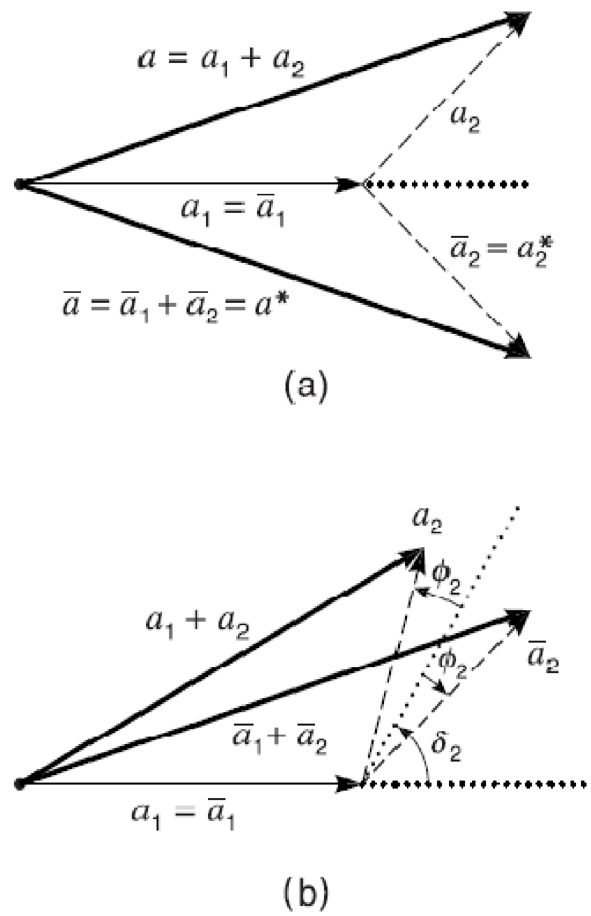

Mixing-induced *CP* violation

- *CP* violation in interference between mixing and decay
- Occurs in decays of neutral *B* mesons to *CP* eigenstates
- Since it depends on *B*-mixing it is a time-dependent effect
- Necessitates measurement of separation of *B* vertices and tag flavour

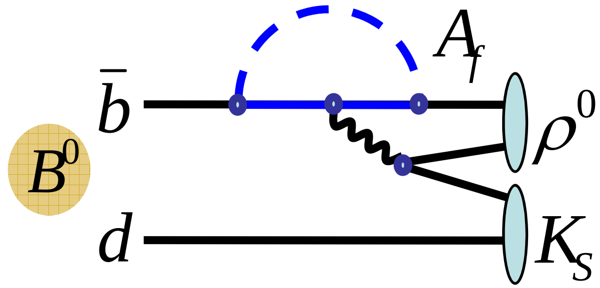

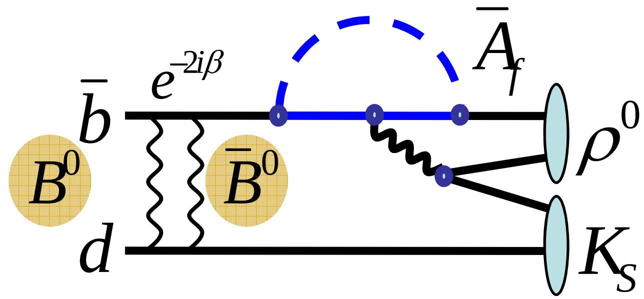

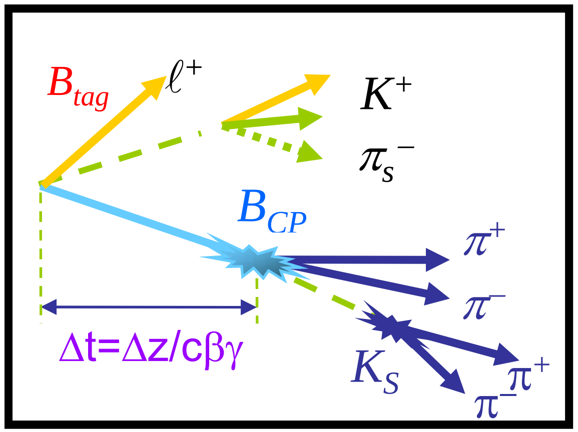

Analysis Variables – Topological

- Light quark continuum cross section ~3x $b\bar{b}$
- *B* mesons produced almost at rest since just above threshold
- Use event topology to discriminate
- Combine variables in an MVA, e.g. Fisher, Neural Network or Decision Tree

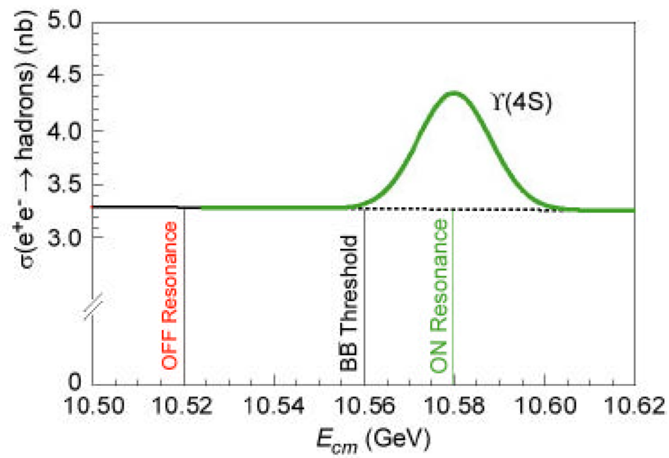

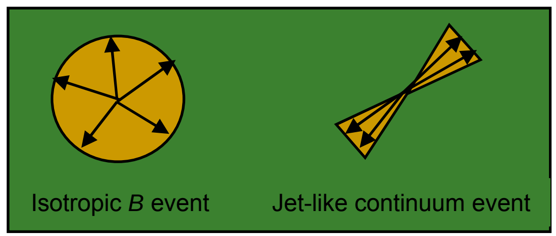

Analysis Variables – Kinematic

Make use of precision kinematic information from the beams.

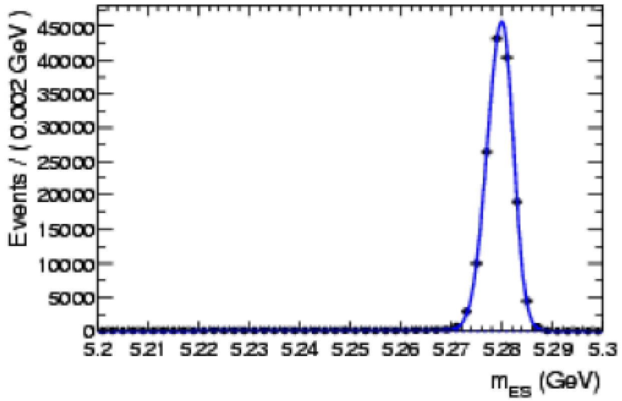

Characteristic Signal Distributions

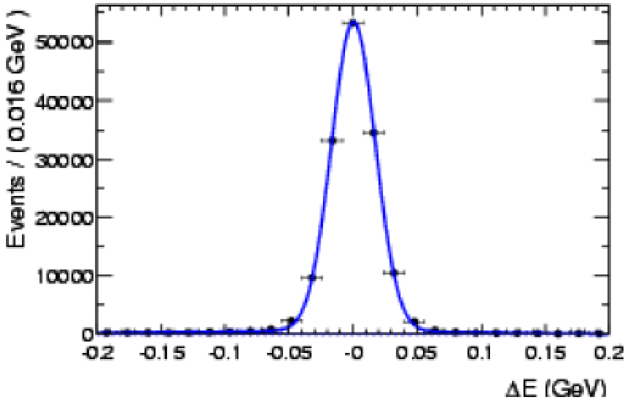

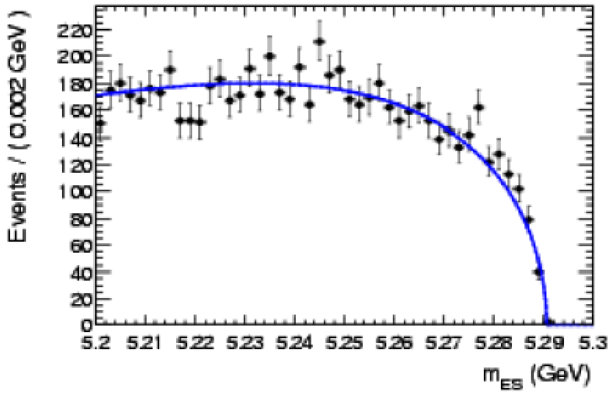

Characteristic Continuum Distributions

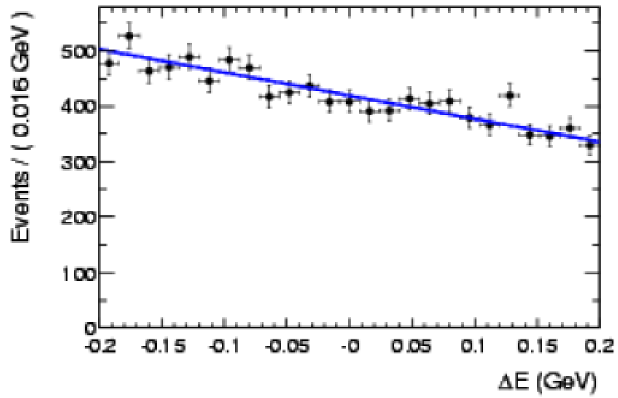

$$m_{ES} = \sqrt{E_{beam}^{*2} - p_B^{*2}}$$

$$\Delta E = E_B^* - E_{beam}^*$$

Search for $B^+ \to K^+K^+\pi^-$ and $B^+ \to K^-\pi^+\pi^+$

- Highly suppressed in the Standard Model
  - BFs of only 10^{-11} and 10^{-14} respectively
  - Significant signals would be clear sign of new physics
- Extended maximum likelihood fit to m_{ES}, ΔE and a Neural Network of topological variables
- Fit includes signal, continuum background and 5 B-background categories

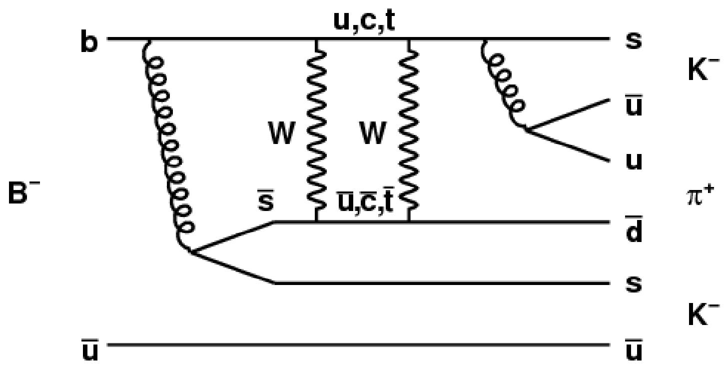

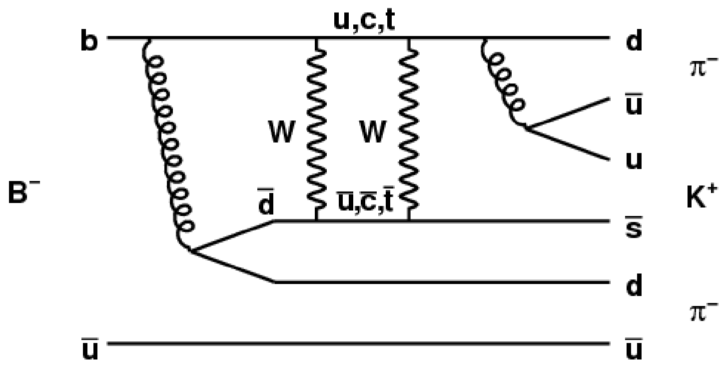

Search for $B^+ \rightarrow K^+K^+\pi^-$ and $B^+ \rightarrow K^-\pi^+\pi^+$

- No significant signals seen in either channel
- Upper limits calculated using Feldman-Cousins method, including systematic uncertainties
- Calculated upper limits are 1.6×10^{-7} and 9.5×10^{-7} respectively
- Improvements of approx factor 8 and 2 respectively
- Results published as rapid communication in Phys. Rev. **D78**, 091102 (2008)

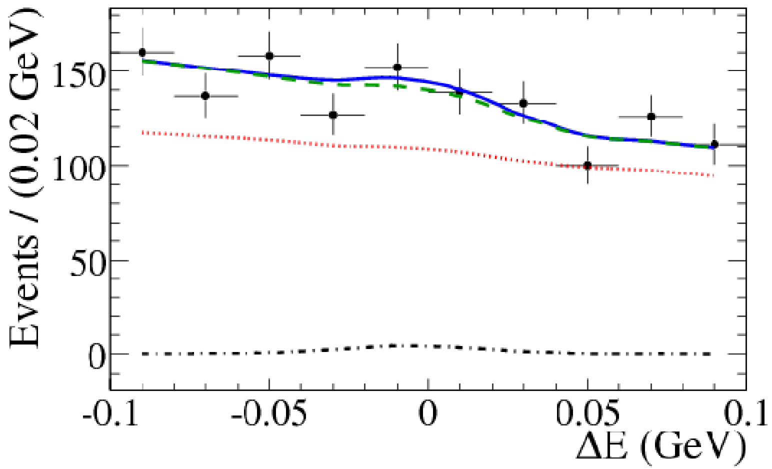

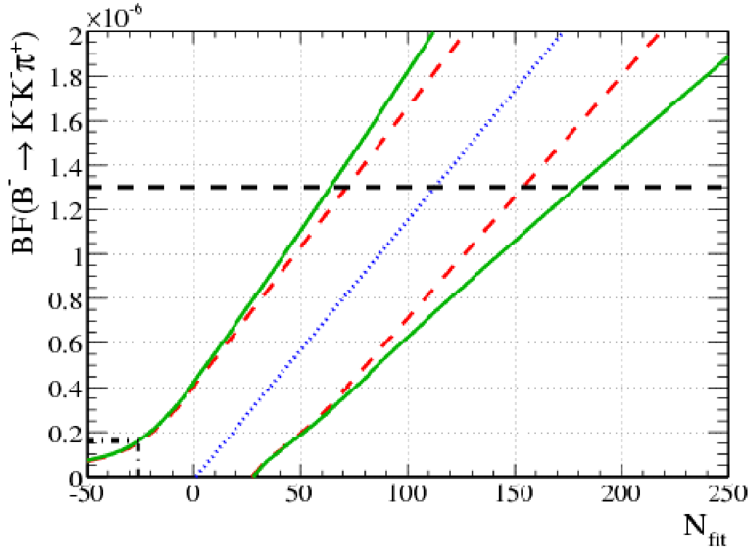

Introduction to Dalitz-plot analysis

- Dalitz plot (DP) is a 2D visualisation of the complete phase space for decays of a spin-0 particle into 3 spin-0 particles (i,j,k)
  - e.g. decays of a *B* meson into combinations of $\pi^{\pm}$, π^0, $K^{\pm}$, K^0, η, η' etc.
- Any point in the DP must satisfy

$$m_B^2 + m_i^2 + m_j^2 + m_k^2 = m_{ij}^2 + m_{ik}^2 + m_{jk}^2$$

- Traditionally plotted as m^2_{ik} vs. m^2_{jk}
- Purely phase-space decays would uniformly populate the DP

An example Dalitz plot

- Resonances appear as bands of events in the Dalitz plot
- Position and size of band related to mass and width of resonance
- Resonance spin determines distribution of events along the band
- Exact pattern of events in Dalitz plot determined by interference between the various contributing states

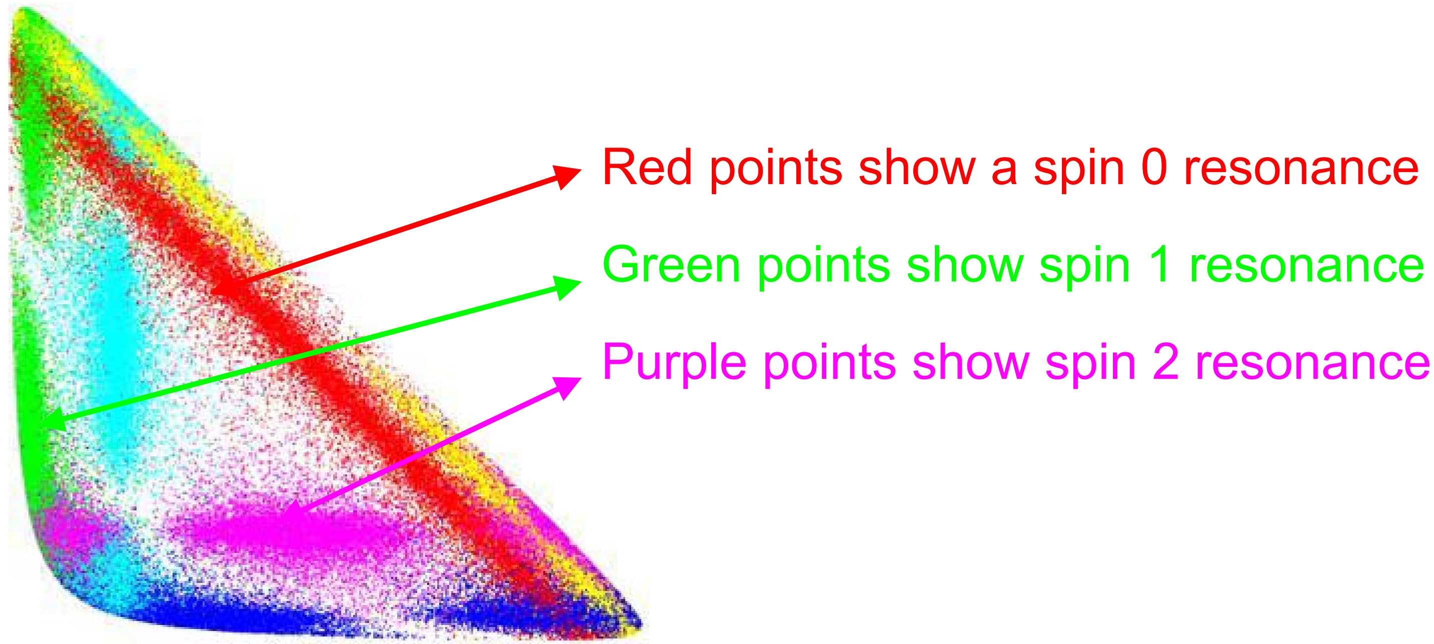

CP Violation in Dalitz plots

- Measurement of relative phases of intermediate states gives greater sensitivity to *CP* violation effects e.g.
  - Direct *CP* violation with only relative weak phase
  - Sensitivity to both sin(2β) and cos(2β) in time-dependent measurements
  - Sensitivity to γ by combining measurements
- Comes at the cost of model dependence

Isobar Model

- Model the complete 3-body decay as a sum of contributing amplitudes

$$A = c_{\mathrm{NR}} e^{i\theta_{\mathrm{NR}}} + \sum_{\mathrm{res}} c_{\mathrm{res}} e^{i\theta_{\mathrm{res}}} F_{\mathrm{res}}$$

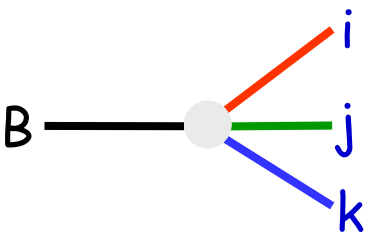

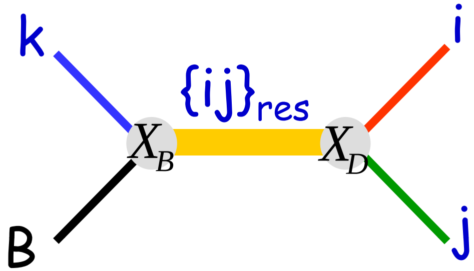

- Both nonresonant and resonant amplitudes
- *F* = resonance dynamics
- *c* and θ are relative magnitudes and phases

Resonance Dynamics

- Describe resonances by a product of factors

$$F = R \times X_B \times X_D \times T$$

  - R = mass dependence, e.g. Breit-Wigner
  - X = Blatt-Weisskopf form factors for resonance production and decay
  - T = angular factor, e.g. Zemach formalism
- Together these determine the variation of the magnitude and phase over the Dalitz plot

Dalitz-plot analysis of charmless 3-body decays

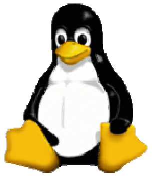

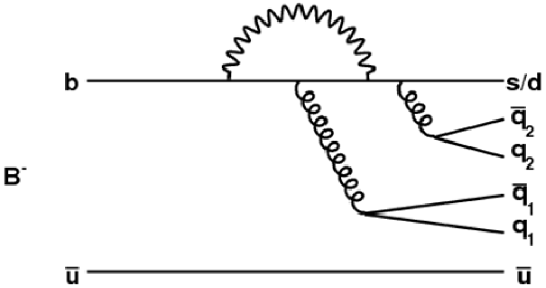

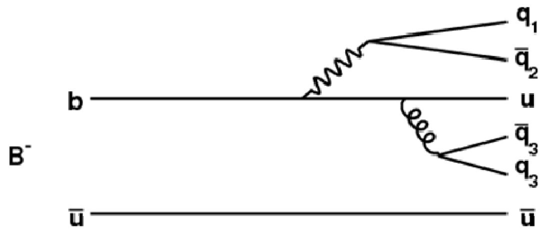

- Rich structure of possible intermediate resonant states in the Dalitz plot, e.g. K^*, ϕ, ρ, f_0
  - Interference allows measurement of relative phases
- Contributions from $b \to s$ (penguin), $b \to u$ (tree) and $b \to d$ (penguin) processes
  - Relative weak phase (γ) between tree and penguins
  - Possibility for direct *CP* violation

$B^+ \rightarrow K^+\pi^+\pi^-$

Introduction to $B^+ \rightarrow K^+\pi^+\pi^-$

- Theoretical prediction and previous experimental hints of large A_{CP} in $B^+ \rightarrow \rho^0 K^+$
  - Both tree and penguin diagrams contribute
- No *CP* asymmetry expected in $B^+ \rightarrow K^{*0}\pi^+$
  - Any observation would be sign of new physics
- DP analysis is sensitive to both magnitude and phase differences
- Highest (BF x ε) of all $K\pi\pi$ modes
  - Knowledge of signal DP model determined here can feed into analyses of other modes
- BABAR results from 383 million BB pairs published in Phys. Rev. **D78**, 012004 (2008)

Details of $K^+\pi^+\pi^-$ Signal Model

- Signal model contains:
  - $K^{*0}(892)$ – Relativistic Breit-Wigner
  - $K\pi$ S-wave – LASS
  - $K_2^{*0}(1430)$ – RBW
  - $\rho^0(770)$ – RBW
  - $\omega(782)$ – RBW
  - $f_0(980)$ – Flatté
  - $f_2(1270)$ – RBW
  - "$f_X(1300)$" – RBW (m and Γ consistent with $f_0(1500)$)
  - χ_{c0} – RBW
  - Phase-space nonresonant

Plots from $K^+\pi^+\pi^-$ DP Fit

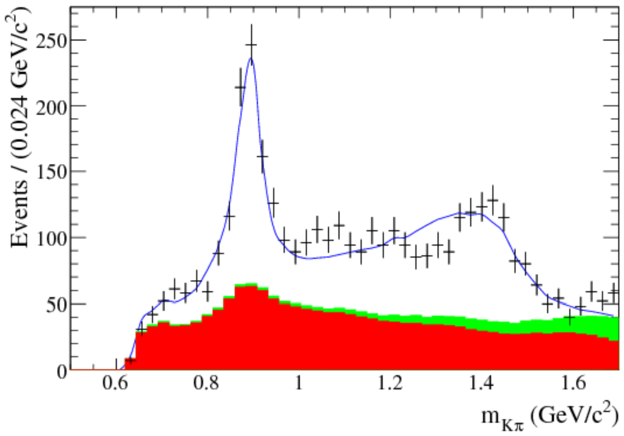

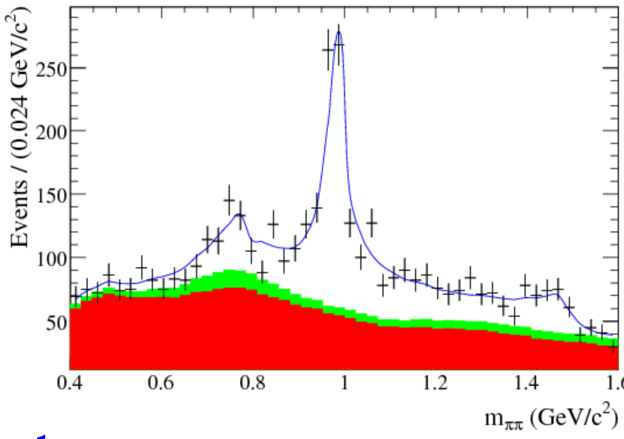

Total Fit Result

Continuum background

BB background

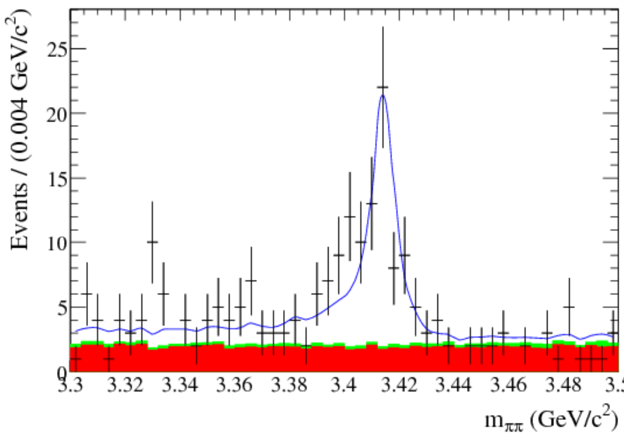

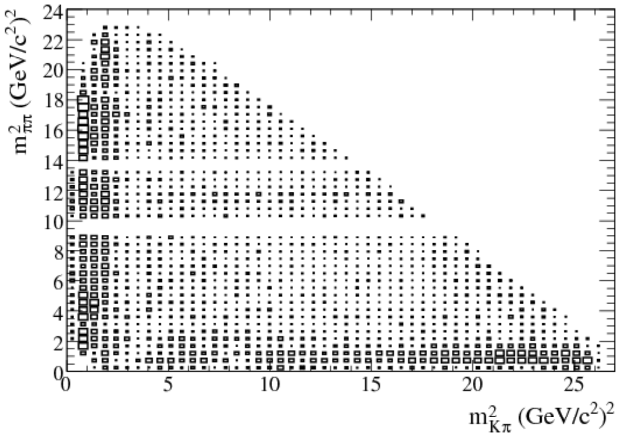

Fit Results from $K^+\pi^+\pi^-$ Analysis

Mode	Fit Fraction (%)	$\mathcal{B}(B^+ \to \text{Mode})(10^{-6})$	A_{CP} (%)	DCPV Sig.
$K^+\pi^-\pi^+$ Total		$54.4 \pm 1.1 \pm 4.5 \pm 0.7$	$2.8 \pm 2.0 \pm 2.0 \pm 1.2$	
$K^{*0}(892)\pi^+;\ K^{*0}(892) \to K^+\pi^-$	$13.3 \pm 0.7 \pm 0.7\,^{+0.4}_{-0.9}$	$7.2 \pm 0.4 \pm 0.7\,^{+0.3}_{-0.5}$	$+3.2 \pm 5.2 \pm 1.1\,^{+1.2}_{-0.7}$	0.9σ
$(K\pi)^{*0}_0\pi^+;\ (K\pi)^{*0}_0 \to K^+\pi^-$	$45.0 \pm 1.4 \pm 1.2\,^{-12.9}_{-0.2}$	$24.5 \pm 0.9 \pm 2.1\,^{+7.0}_{-1.1}$	$+3.2 \pm 3.5 \pm 2.0\,^{+2.7}_{-1.9}$	1.2σ
$\rho^0(770)K^+;\ \rho^0(770) \to \pi^+\pi^-$	$6.54 \pm 0.81 \pm 0.58\,^{+0.69}_{-0.26}$	$3.56 \pm 0.45 \pm 0.43\,^{+0.38}_{-0.15}$	$+44 \pm 10 \pm 4\,^{+5}_{-13}$	3.7σ
$f_0(980)K^+;\ f_0(980) \to \pi^+\pi^-$	$18.9 \pm 0.9 \pm 1.7\,^{+2.8}_{-0.6}$	$10.3 \pm 0.5 \pm 1.3\,^{+1.5}_{-0.4}$	$-10.6 \pm 5.0 \pm 1.1\,^{+3.4}_{-1.0}$	1.8σ
$\chi_{c0}K^+;\ \chi_{c0} \to \pi^+\pi^-$	$1.29 \pm 0.19 \pm 0.15\,^{+0.12}_{-0.03}$	$0.70 \pm 0.10 \pm 0.10\,^{+0.06}_{-0.02}$	$-14 \pm 15 \pm 3\,^{+1}_{-5}$	0.5σ
$K^+\pi^-\pi^+$ nonresonant	$4.5 \pm 0.9 \pm 2.4\,^{+0.6}_{-1.5}$	$2.4 \pm 0.5 \pm 1.3\,^{+0.3}_{-0.8}$	—	—
$K_2^{*0}(1430)\pi^+;\ K_2^{*0}(1430) \to K^+\pi^-$	$3.40 \pm 0.75 \pm 0.42\,^{+0.99}_{-0.13}$	$1.85 \pm 0.41 \pm 0.28\,^{+0.54}_{-0.08}$	$+5 \pm 23 \pm 4\,^{+18}_{-7}$	0.2σ
$\omega(782)K^+;\ \omega(782) \to \pi^+\pi^-$	$0.17 \pm 0.24 \pm 0.03\,^{+0.05}_{-0.08}$	$0.09 \pm 0.13 \pm 0.02\,^{+0.03}_{-0.04}$	—	—
$f_2(1270)K^+;\ f_2(1270) \to \pi^+\pi^-$	$0.91 \pm 0.27 \pm 0.11\,^{+0.24}_{0.17}$	$0.50 \pm 0.15 \pm 0.07\,^{+0.13}_{0.09}$	$-85 \pm 22 \pm 13\,^{+22}_{2}$	3.5σ
$f_X(1300)K^+;\ f_X(1300) \to \pi^+\pi^-$	$1.33 \pm 0.38 \pm 0.86\,^{+0.04}_{-0.14}$	$0.73 \pm 0.21 \pm 0.47\,^{+0.02}_{-0.08}$	$+28 \pm 26 \pm 13\,^{+7}_{-5}$	0.6σ

First error is statistical, second systematic and third model-dependent.
Significance of DCPV is statistical only.

Total NR branching fraction = $(9.3 \pm 1.0 \pm 1.2\,^{+6.7}_{-0.4} \pm 1.2) \times 10^{-6}$

$B^+ \rightarrow \rho^0 K^+$ Direct *CP* Asymmetry

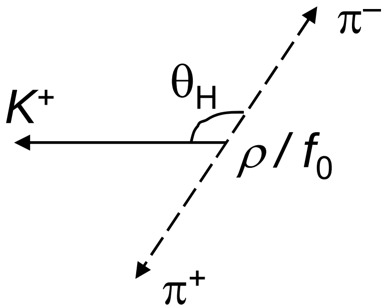

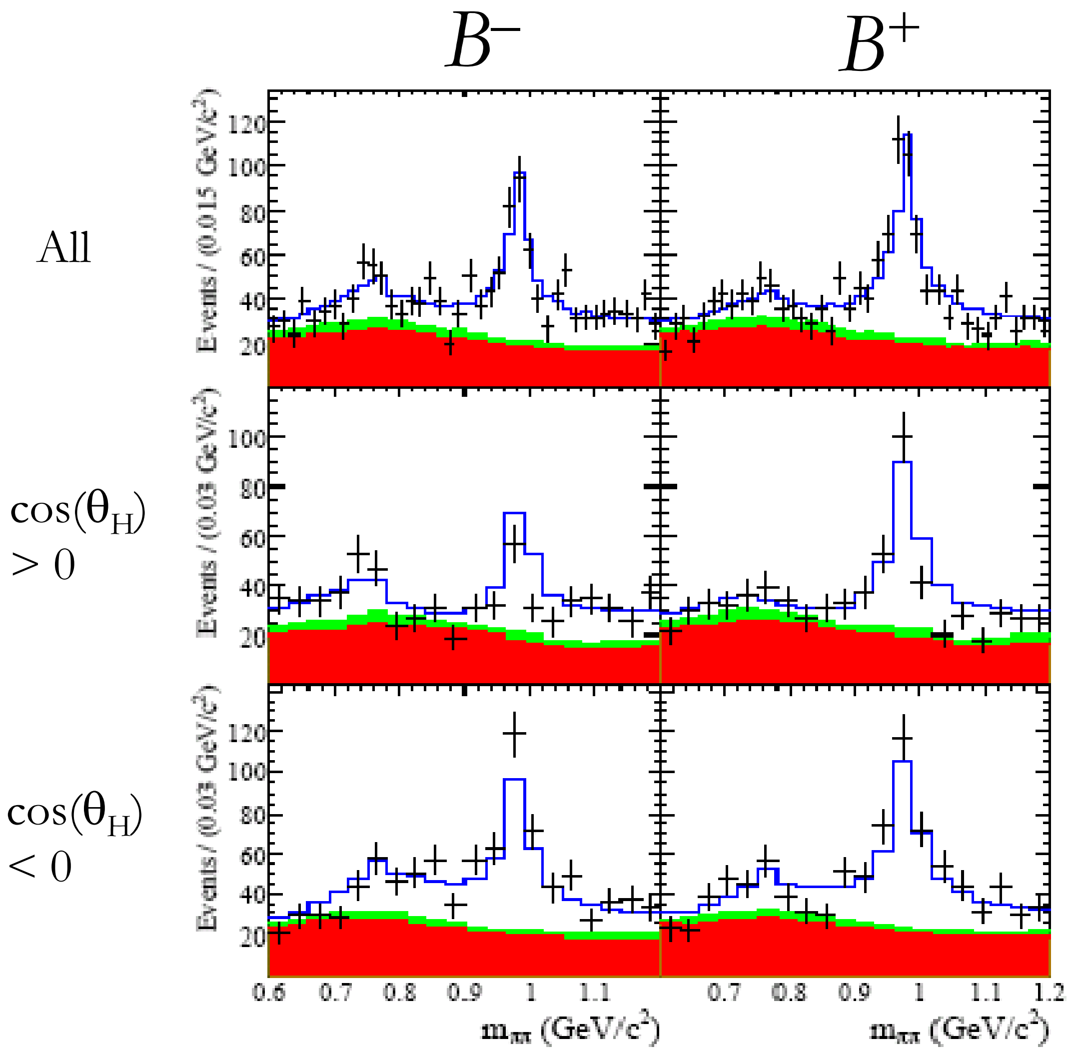

Determining *γ* from *K*ππ

Determining γ from $K\pi\pi$ DPs

- Much recent theoretical activity in this area
- Main method involves $K^+\pi^-\pi^0$ and $K_S\pi^+\pi^-$ DPs
  - Ciuchini et al., Phys. Rev. D74, 051301 (2006)
  - Gronau et al., Phys. Rev. D75, 014002 (2007)
  - Gronau et al., Phys. Rev. D77, 057504 (2008) and D78, 017505 (2008)
- Other methods use $K_S\pi^+\pi^0$; $K^+\pi^+\pi^-$ & $K_S\pi^+\pi^-$; and B_s decays to $K^+\pi^-\pi^0$ & $K_S\pi^+\pi^-$
  - Ciuchini et al., Phys. Rev. D74, 051301 (2006)
  - Bediaga et al., Phys. Rev. D76, 073011 (2007)
  - Ciuchini et al., Phys. Lett. B645, 201 (2007)

Determining γ from $K\pi\pi$ DPs

- Method from Ciuchini et al. and Gronau et al.
- Use $B \rightarrow K^*\pi$ modes to form isospin triangles
- $A_{ij} = A(B^0 \rightarrow K^{*i}\pi^j)$
- $\Phi_{3/2} = \gamma$ up to correction from EW penguins
- The amplitude magnitudes as well as ϕ, $\bar{\phi}$ and $\Delta\phi$ can be measured from Dalitz-plot analyses of $K^+\pi^-\pi^0$ and $K_s\pi^+\pi^-$

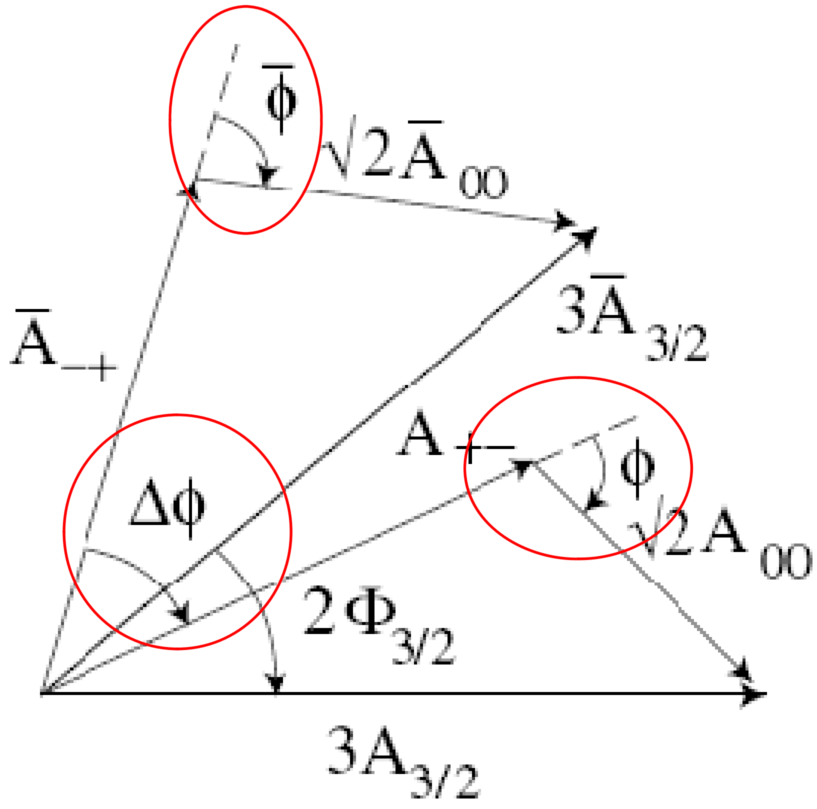

$B^0 \rightarrow K_S\pi^+\pi^-$

Introduction to $B^0 \rightarrow K_S\pi^+\pi^-$

- Phase $\Delta\phi$ can be determined from this DP from interference between:
  - $K^{*+}\pi^-$ and $\rho^0 K_S$ in the B^0 decay
  - $K^{*-}\pi^+$ and $\rho^0 K_S$ in the $\bar{B}^0$ decay
- This measurement does not require tagging or time-dependent analysis
- However, time-dependent analysis also allows measurements of β_{eff} from $\rho^0 K_S$, $f_0 K_S$

Time-dependent Dalitz-plot Analysis

- Combining both techniques leads to a very complex PDF
- Each point in the DP can have a different time evolution
  - The different signal model components interfere as normal
  - In addition the B^0 and $\overline{B}^0$ amplitudes interfere through mixing
- Effects of mis-tagging and the detector resolution on Δt measurement have to be taken into account

$$
\begin{aligned}
\mathcal{L}_n^{sig}(m_+^2, m_-^2, \Delta t, q_{\rm tag}) \; = \; & \frac{1}{\mathcal{N}} \sum_c f_c \frac{e^{-|\Delta t|/\tau_{B^0}}}{4\tau_{B^0}} \times \\
& \left[\left(|\mathcal{A}|^2 + |\overline{\mathcal{A}}|^2 \right) \left(1 + q_{\rm tag} \frac{\Delta D^c}{2} \right) \right. \\
& - q_{\rm tag} \left\langle D \right\rangle^c \left(|\mathcal{A}|^2 - |\overline{\mathcal{A}}|^2 \right) \cos\left(\Delta m_d \Delta t \right) \\
& \left. + q_{\rm tag} \left\langle D \right\rangle^c 2{\rm Im}\left[\overline{\mathcal{A}} \mathcal{A}^* e^{-i\phi_{mix}} \right] \sin\left(\Delta m_d \Delta t \right) \right],
\end{aligned}
$$

Details of $K_S\pi^+\pi^-$ Signal Model

- Signal model contains:
  - $K^{*+}(892)$ – Relativistic Breit-Wigner
  - $K\pi$ S-wave – LASS
  - $\rho^0(770)$ – Gounaris-Sakurai
  - $f_0(980)$ – Flatté
  - $f_2(1270)$ – RBW
  - "$f_X(1300)$" – RBW (m and Γ consistent w/ $f_0(1500)$)
  - χ_{c0} – RBW
  - Phase-space nonresonant

Plots from $K_S\pi^+\pi^-$ DP Fit

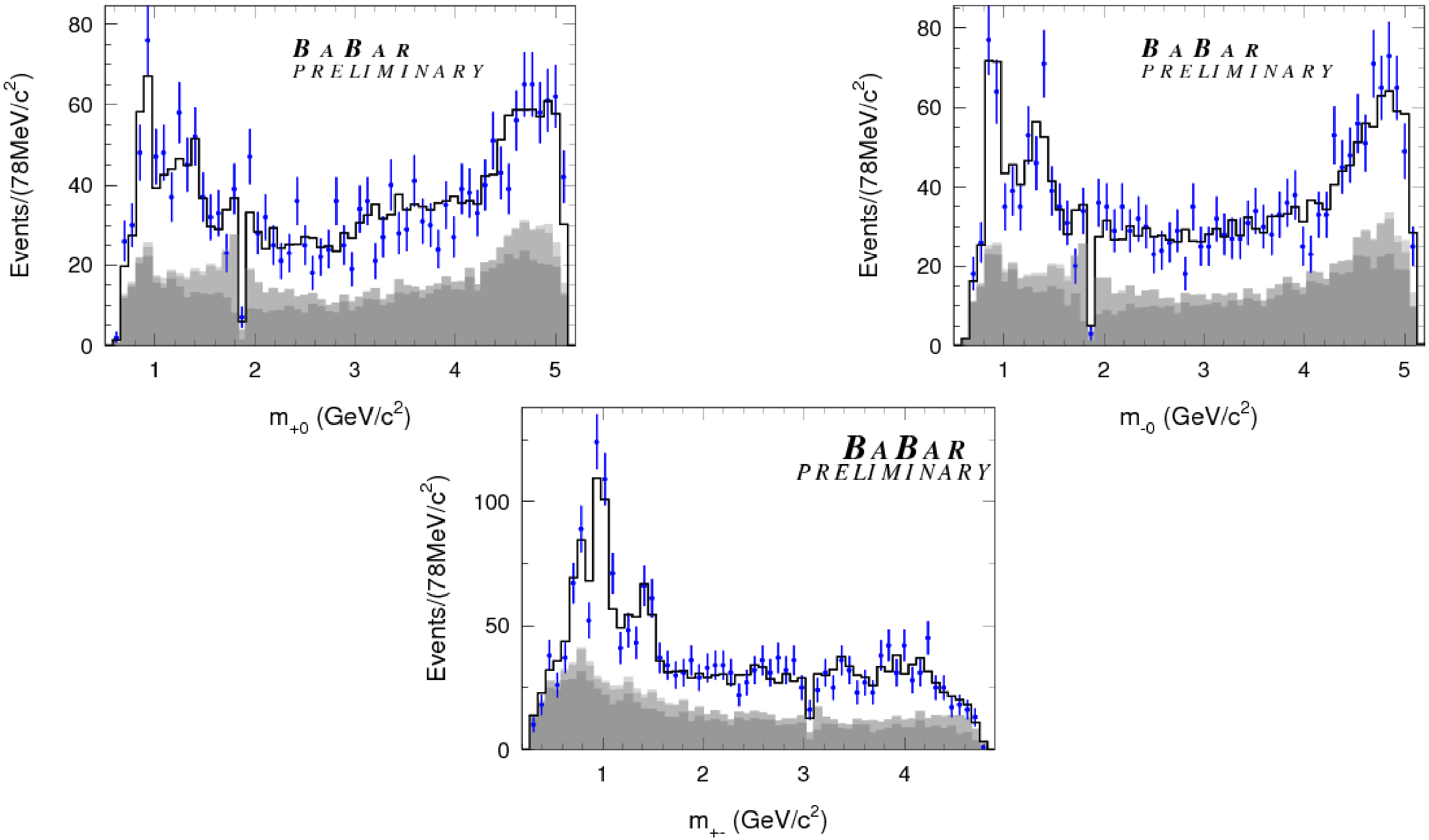

Fit Results – $B^0 \to K_S\pi^+\pi^-$

- BABAR preliminary results from 383 million $B\bar{B}$ give:
  $2\beta_{eff}(f_0K_S) = (89 \pm 22 \pm 5 \pm 8)^\circ$
  $2\beta_{eff}(\rho^0K_S) = (37 \pm 19 \pm 5 \pm 6)^\circ$
- Errors are stat, syst, model
- Both results are compatible with measurements from charmonium
- Conference paper: arXiv:0708.2097 [hep-ex]

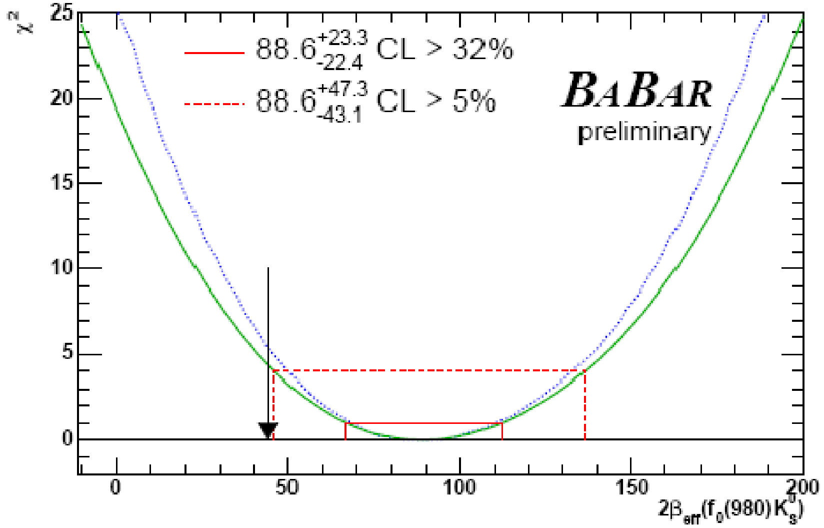

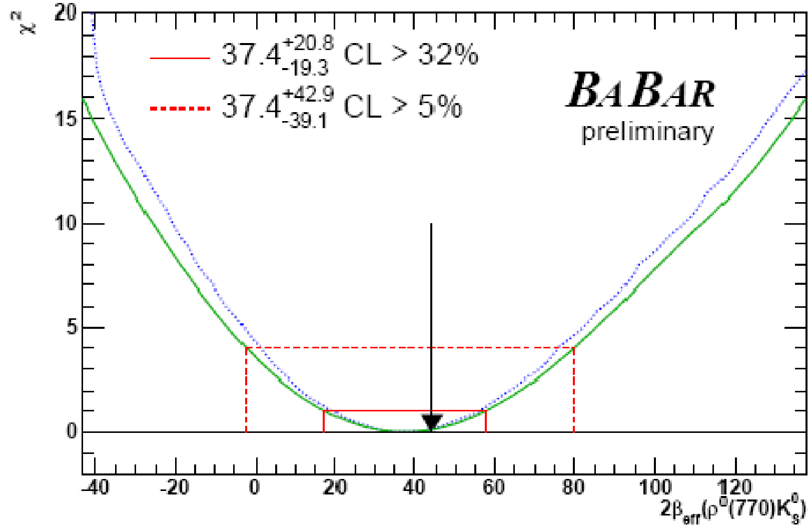

Fit Results – $B^0 \rightarrow K_S\pi^+\pi^-$

- BABAR preliminary result:
  $\Delta\phi = (-164 \pm 24 \pm 12 \pm 15)°$
- Errors are stat, syst, model
- This phase difference includes the $B^0\bar{B}^0$ mixing phase (-2β)
- Secondary solution excluded at $>3\sigma$

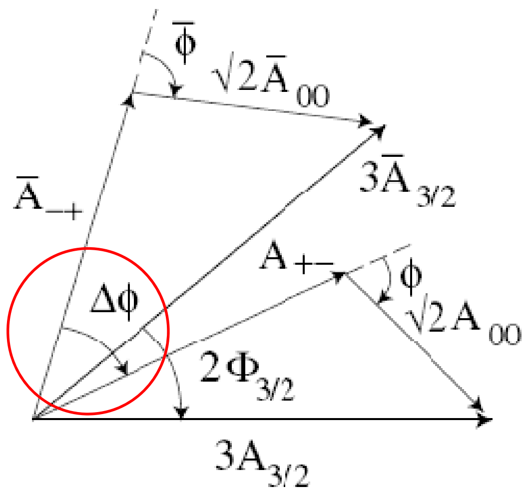

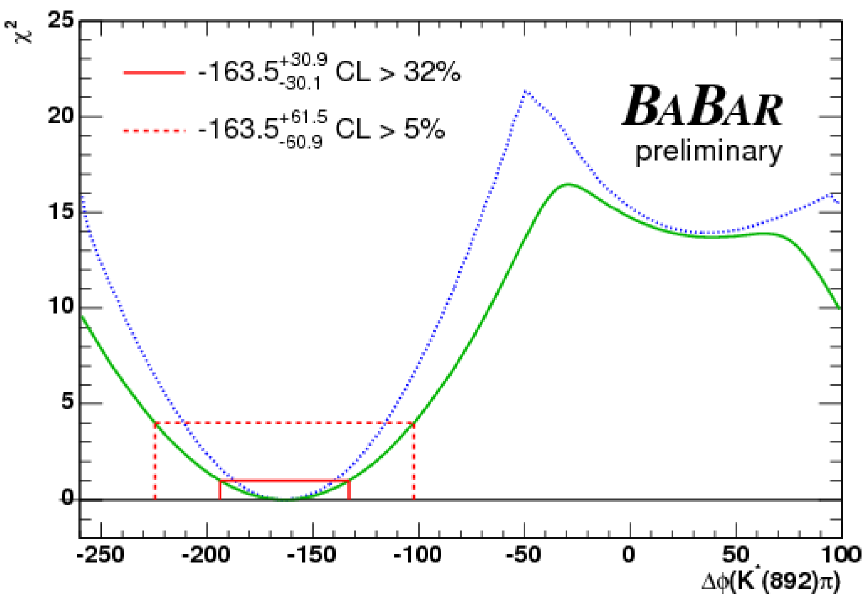

$$B^0 \to K^+\pi^-\pi^0$$

Introduction to $B^0 \to K^+\pi^-\pi^0$

- Can determine the phases ϕ and $\bar{\phi}$ from this Dalitz plot
- Mode is self-tagging (from charge of kaon) so analysis does not involve flavour tagging or time-dependence
- BaBar have results from 232 million BB
  - Also preliminary results from 454 million BB
- Analysis not yet performed by Belle

Details of $K^+\pi^-\pi^0$ Signal Model

- Signal model contains:
  - $K^{*+}(892)$ – Relativistic Breit-Wigner
  - $K^{*0}(892)$ – Relativistic Breit-Wigner
  - $(K\pi)^+$ S-wave – LASS
  - $(K\pi)^0$ S-wave – LASS
  - $\rho^-(770)$ – Gounaris-Sakurai
  - Phase-space nonresonant

Plots from $K^+\pi^-\pi^0$ DP Fit

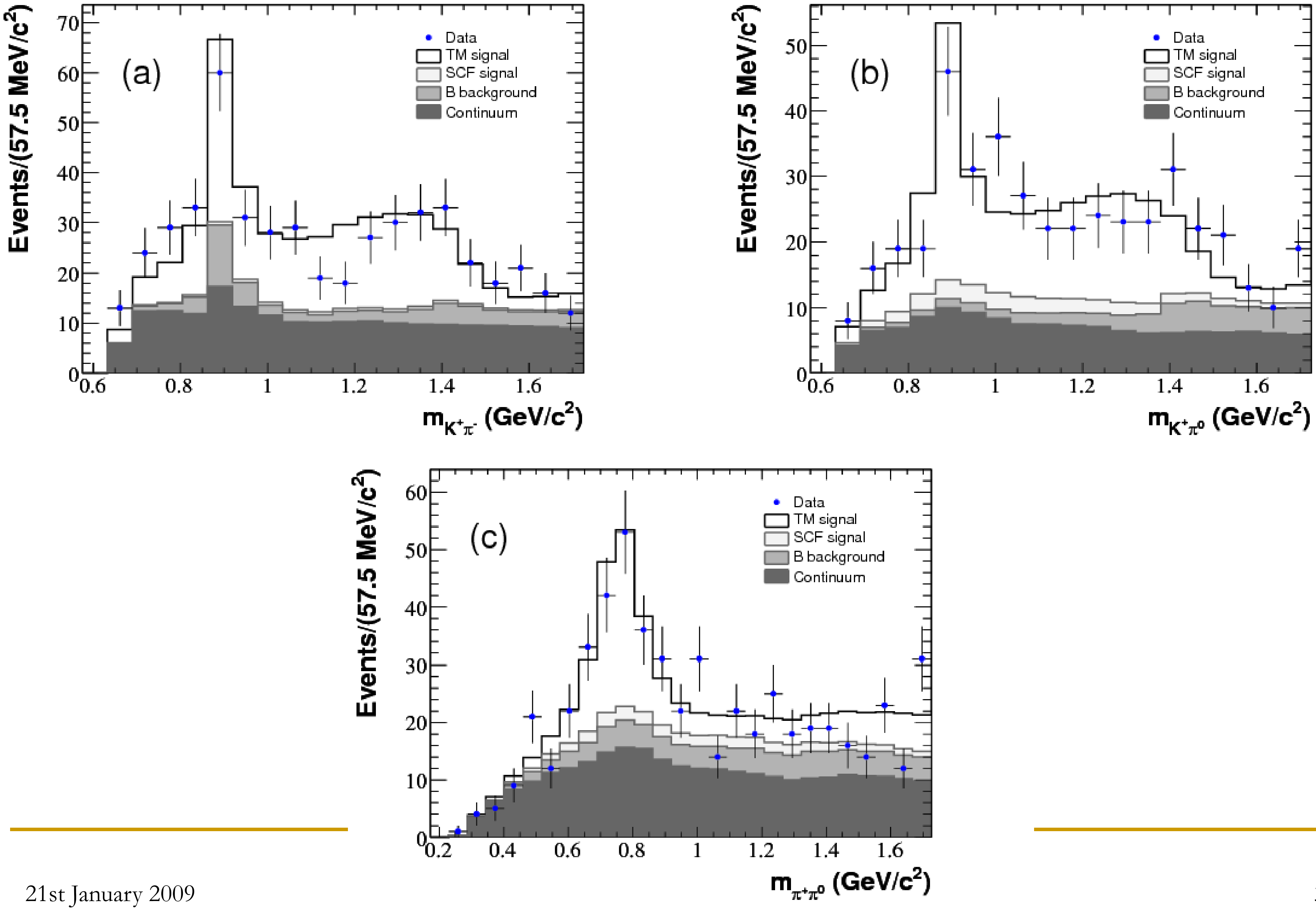

Fit Results – $B^0 \to K^+\pi^-\pi^0$

- BABAR results from 232 million BB pairs published in:
  - Phys. Rev. **D78**, 052005 (2008)
- Scans opposite show the results for ϕ and $\bar{\phi}$
- Presence of multiple solutions reduces precision of constraint
- Preliminary BABAR results on 454 million BB indicate much better separation between solutions
  - Likelihood scans of phase differences not yet completed
  - arXiv:0807.4567 [hep-ex]

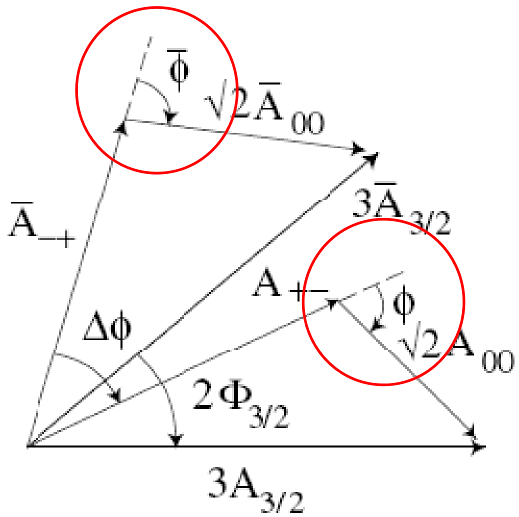

Fit Results – $B^0 \rightarrow K^+\pi^-\pi^0$

- BaBar results from 232 million BB pairs published in:
  - Phys. Rev. **D78**, 052005 (2008)
- Scans opposite show the results for ϕ and $\bar{\phi}$
- Presence of multiple solutions reduces precision of constraint
- Preliminary BaBar results on 454 million BB indicate much better separation between solutions
  - Likelihood scans of phase differences not yet completed
  - arXiv:0807.4567 [hep-ex]

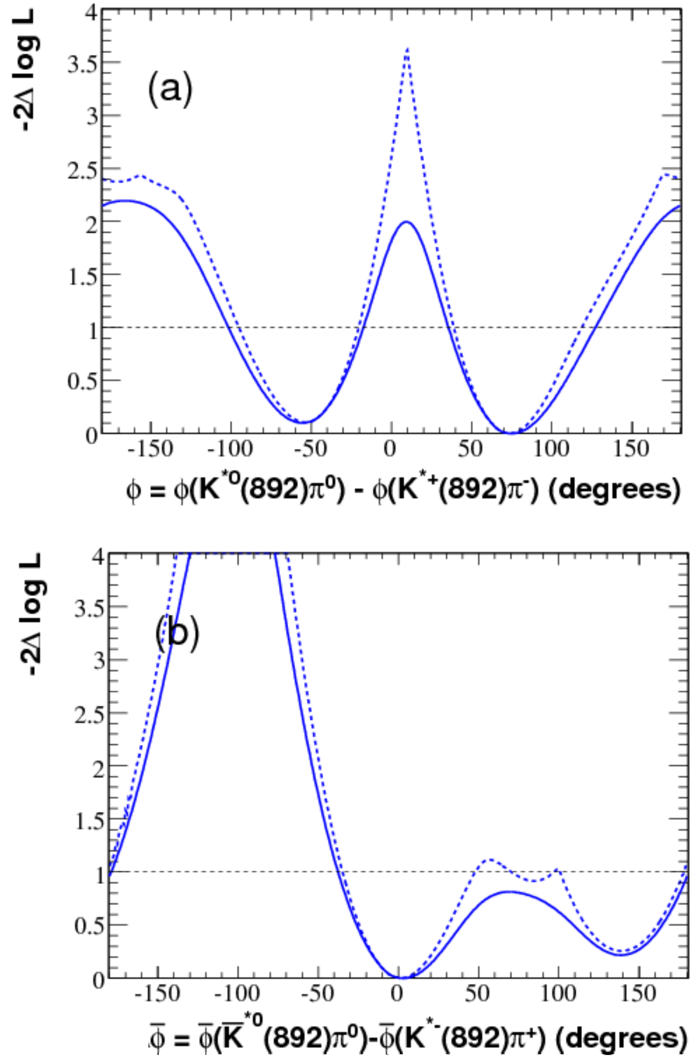

Constraining γ

Constraining γ

- BABAR results from $K_S\pi^+\pi^-$ (arXiv:0708.2097) and $K^+\pi^-\pi^0$ (arXiv:0711.4417) combined together
  - Gronau et al., Phys. Rev. D77, 057504 (2008) and D78, 017505 (2008)

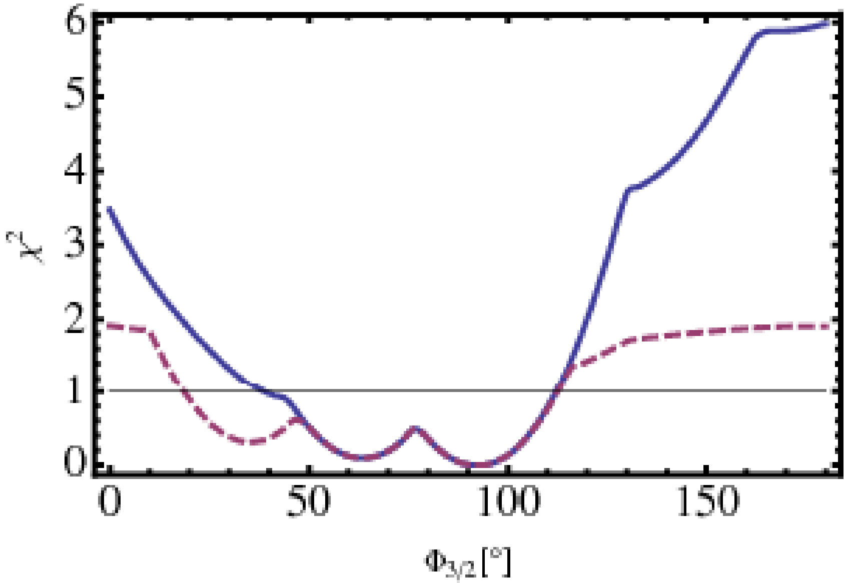

Dotted purple line – unconstrained $|R_{3/2}|$
Solid blue line – $0.8 < |R_{3/2}| < 1.2$

$39° < \Phi_{3/2} < 112°$ (68% CL)

Constraining γ

- CKM constraint in presence of EW penguins is:

$$\bar{\eta} = \tan\Phi_{3/2}\left[\bar{\rho} - 0.24 \pm 0.03\right]$$

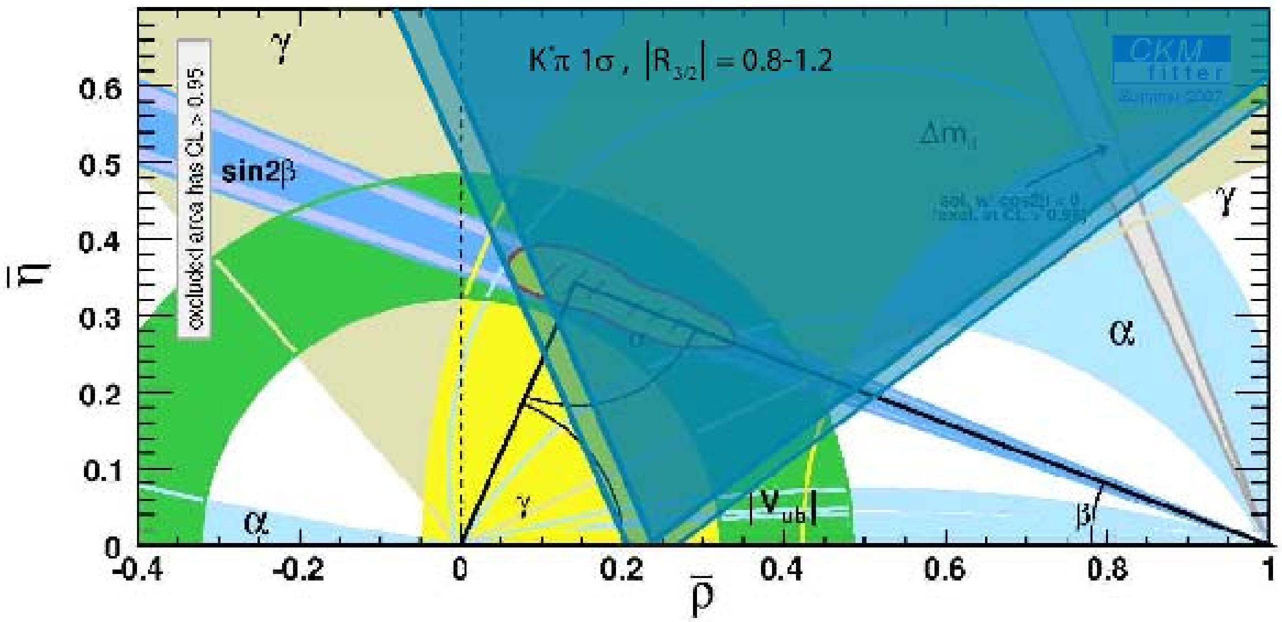

Conclusion

- Charmless 3-body decays of B mesons allow measurements of all 3 Unitarity Triangle angles
  - Not mentioned in this talk – TDDP analysis of $B \rightarrow \pi\pi\pi^0$ allows measurement of α and of KKK_S gives further information on β_{eff}
- The B-factories have reacted quickly to the theoretical developments regarding constraining γ with $B \rightarrow K\pi\pi$ decays
- Results available allow such a constraint to be formed
- Updated results expected soon from BABAR
  - Should help to resolve ambiguities
- Measurements from other K$\pi\pi$ modes, such as $B \rightarrow K_S\pi^+\pi^0$, could help improve the precision
- Future experiments, such as LHCb and a possible Super Flavour Factory, will be able to improve precision of these results

Backup Material

General differences between BABAR and Belle $B \to K\pi\pi$ analyses

- Main difference is in approach to low mass $K\pi$ S-wave
- BABAR use the LASS parameterisation
  - Coherent sum of $K_0^*(1430)$ and effective range nonresonant that is constrained to be unitary
- BABAR analyses also have to include a phase-space NR term to account for NR events above LASS cut-off (~1.8 GeV/c^2)
- Belle use $K_0^*(1430)$ as RBW and exponential shaped NR
- Belle parameterisation often suffers from multiple solutions where the fractions of the $K_0^*(1430)$ are very different
  - Preferred solution can often depend on which other terms are included in the DP model, e.g. $K_2^*(1430)$
- Neither approach is perfect but both seem to allow a pretty good fit to the data
- Does make comparison of results rather tricky
- However, different approaches don't seem to significantly affect results for other modes in the DP, e.g. $\rho^0 K^+$ A_{CP}

Systematic/Model dependence of DCPV in $\rho^0(770)K^+$

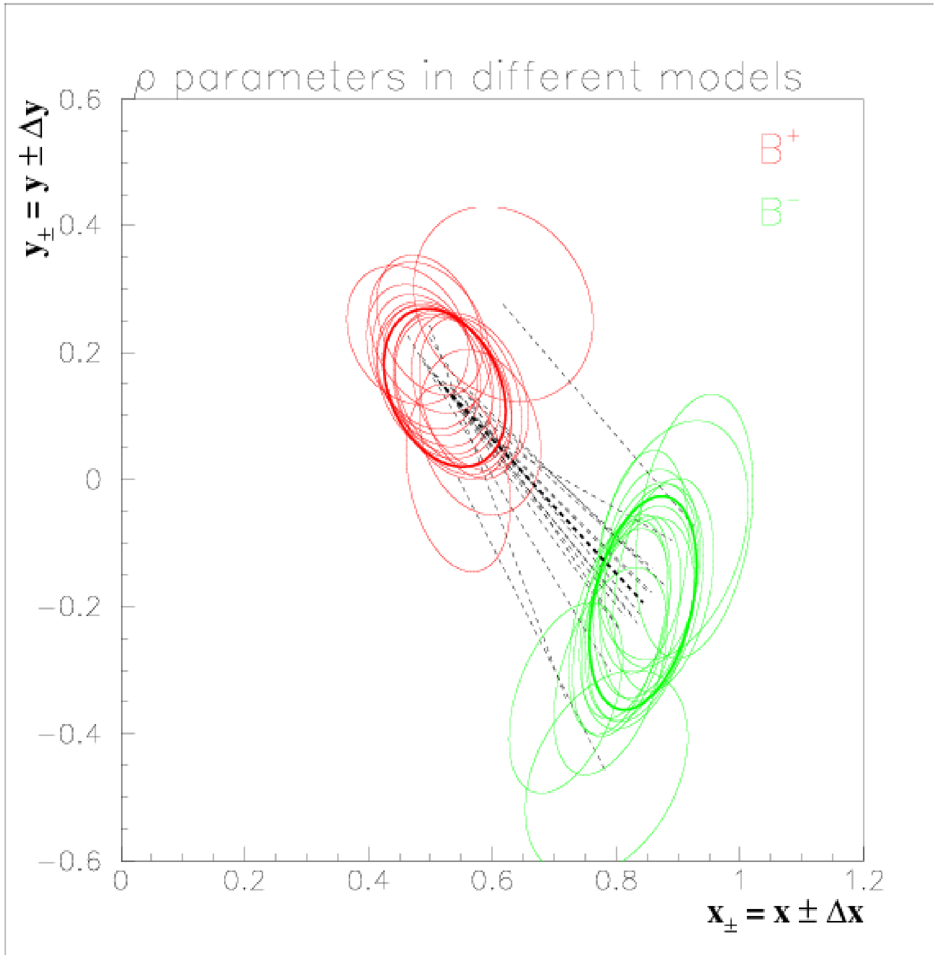

Comparison with Belle – $B^+ \rightarrow K^+\pi^+\pi^-$

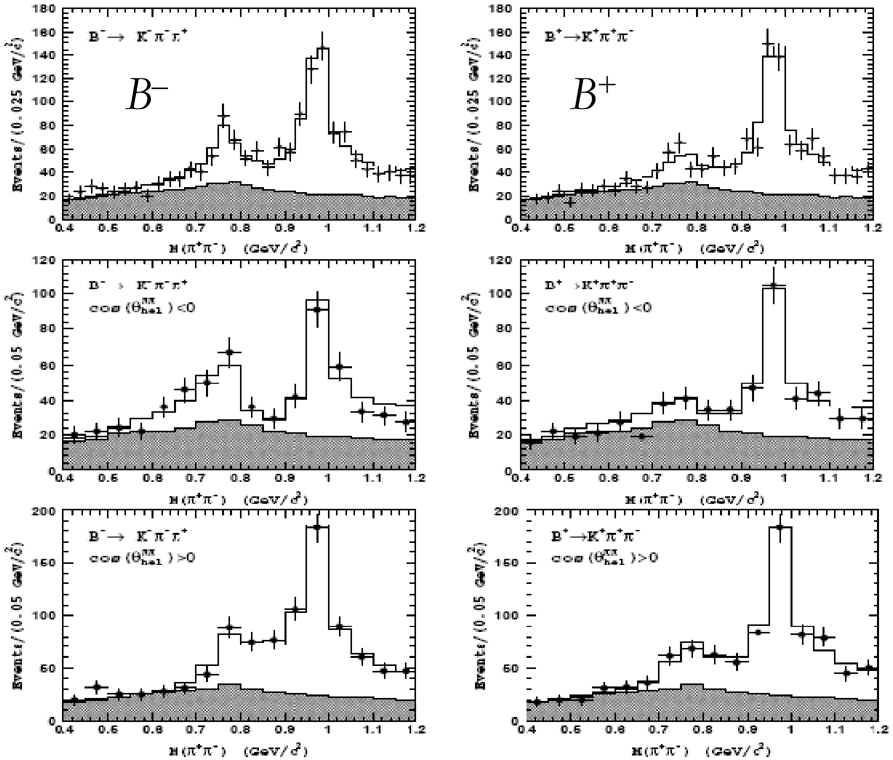

All

$\cos(\theta_H) > 0$

$\cos(\theta_H) < 0$

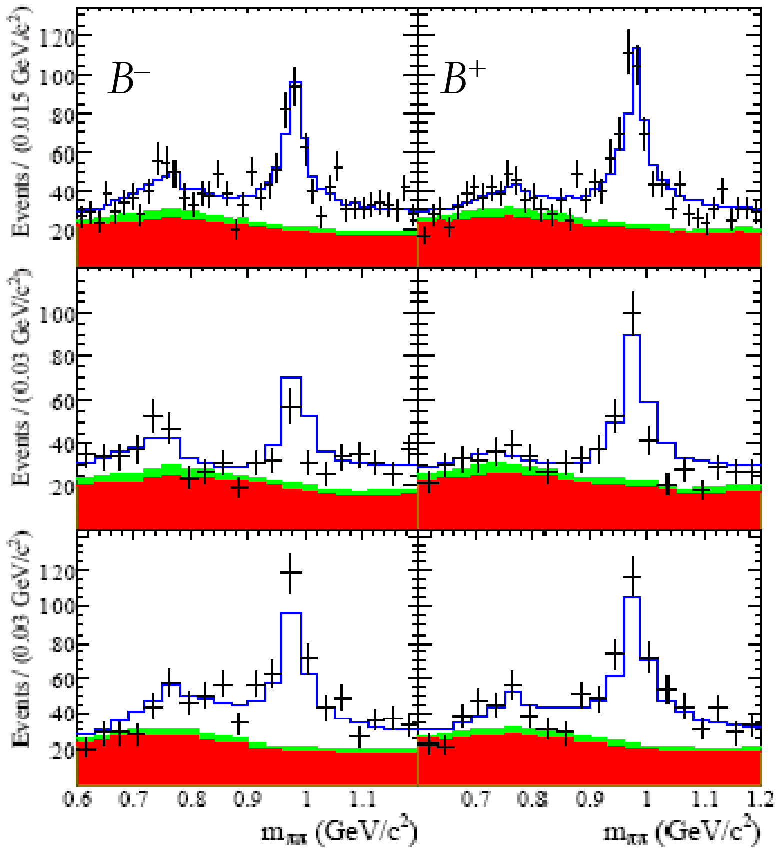

BELLE-CONF-0827 – 657 million BB

$A_{CP}(\rho^0 K^+) = (+41 \pm 10 \pm 3 \pm {}^{3}_{7})\%$

PRD 78, 012004 (2008) – 383 million BB

$A_{CP}(\rho^0 K^+) = (+44 \pm 10 \pm 4 \pm {}^{5}_{13})\%$

Details of BABAR $K_S\pi^+\pi^-$ Analysis

Resonance Name	$\lvert c_\sigma \rvert$	ϕ[degrees]	$\lvert \bar{c}_\sigma \rvert$ ($\lvert \overline{c_{\bar{\sigma}}} \rvert$)	$\bar{\phi}$[degrees]
$f_0(980)K_S^0$	4.0	0.0	2.8 ± 0.7	-88.6 ± 21.3
$\rho^0(770)K_S^0$	0.10 ± 0.02	58.6 ± 16.4	0.09 ± 0.02	21.3 ± 21.2
$f_0(1300)K_S^0$	1.9 ± 0.4	117.6 ± 22.6	1.1 ± 0.3	-15.2 ± 23.8
Nonresonant	3.0 ± 0.6	13.8 ± 14.3	3.7 ± 0.5	-16.2 ± 17.3
$K^{*+}(892)\pi^-$	0.136 ± 0.021	-60.7 ± 18.5	0.113 ± 0.018	102.6 ± 22.9
$K^{*+}(1430)\pi^-$	4.9 ± 0.7	-82.4 ± 16.8	7.1 ± 0.9	79.2 ± 20.5
$f_2(1270)K_S^0$	0.011 ± 0.004	62.9 ± 23.3	0.010 ± 0.003	-73.9 ± 27.8
$\chi_{c0}(1P)K_S^0$	0.34 ± 0.15	68.7 ± 31.1	0.40 ± 0.11	154.5 ± 28.6

Details of Belle $K_S\pi^+\pi^-$ Analysis

- Signal model contains:
  - K^{*+}(892) – Relativistic Breit-Wigner
  - K_0^{*+}(1430) – RBW
  - ρ^0(770) – Gounaris-Sakurai
  - f_0(980) – Flatté
  - f_2(1270) – RBW
  - "f_X(1300)" – RBW (m and Γ consistent w/ f_0(1500))
  - Three exponential shaped NR terms

Comparison with Belle – $B^0 \to K_S\pi^+\pi^-$

- A new Belle preliminary result from 657 million BB:

  $\Delta\phi = (-1 \pm ^{24}_{23} \pm 11 \pm 18)°$

  (errors are stat, syst, model)
- A second, almost degenerate, solution:

  $\Delta\phi = (+15 \pm ^{19}_{20} \pm 11 \pm 18)°$
- Difference between solutions is interference between $K_0^{*\pm}(1430)$ and NR
- These again include the $B^0\bar{B}^0$ mixing phase (-2β)
- Apparent disagreement with the BaBar results

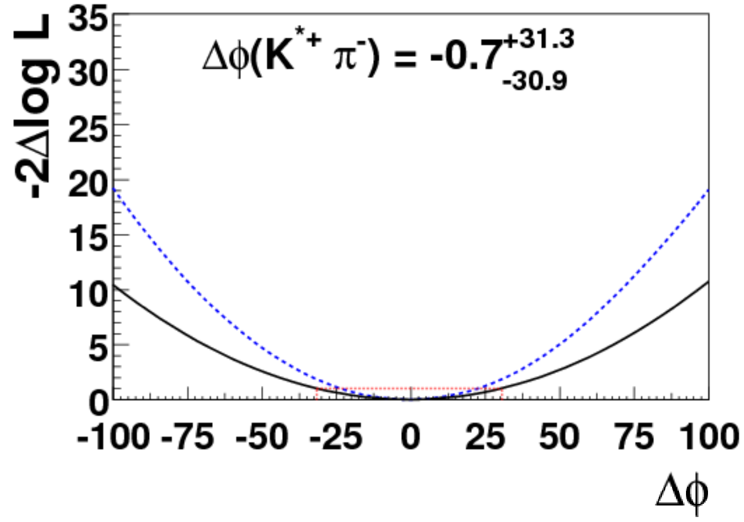

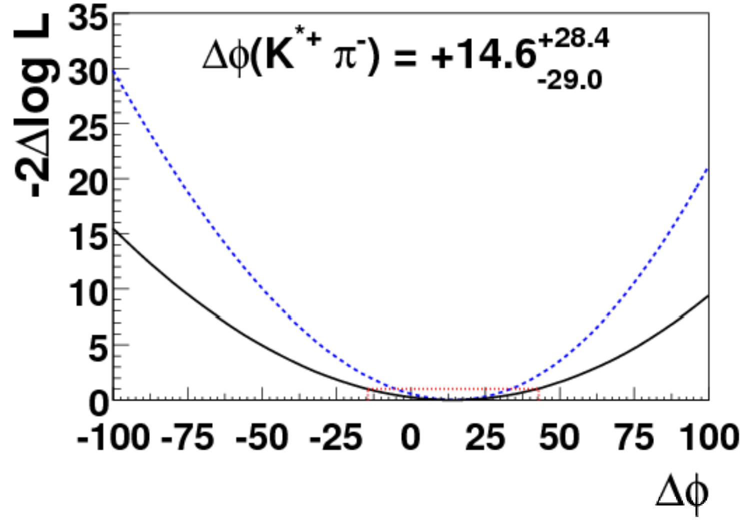

HFAG Averages

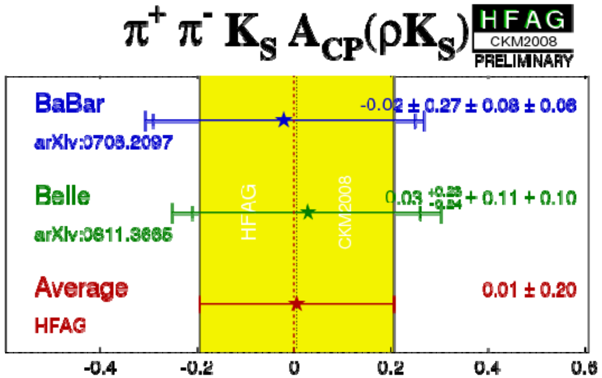

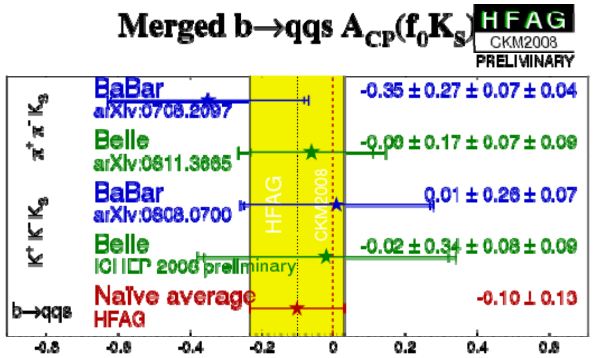

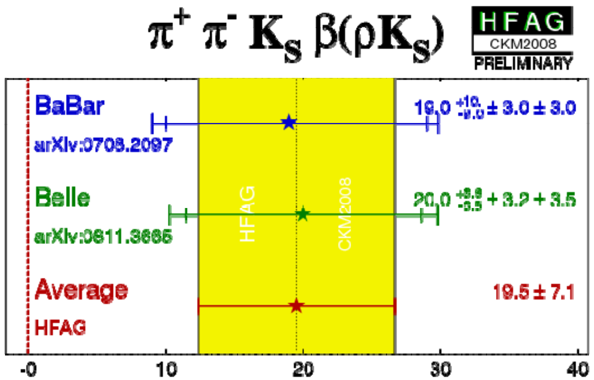

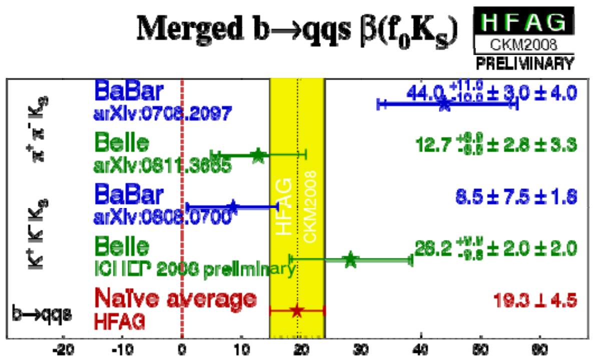

HFAG Averages

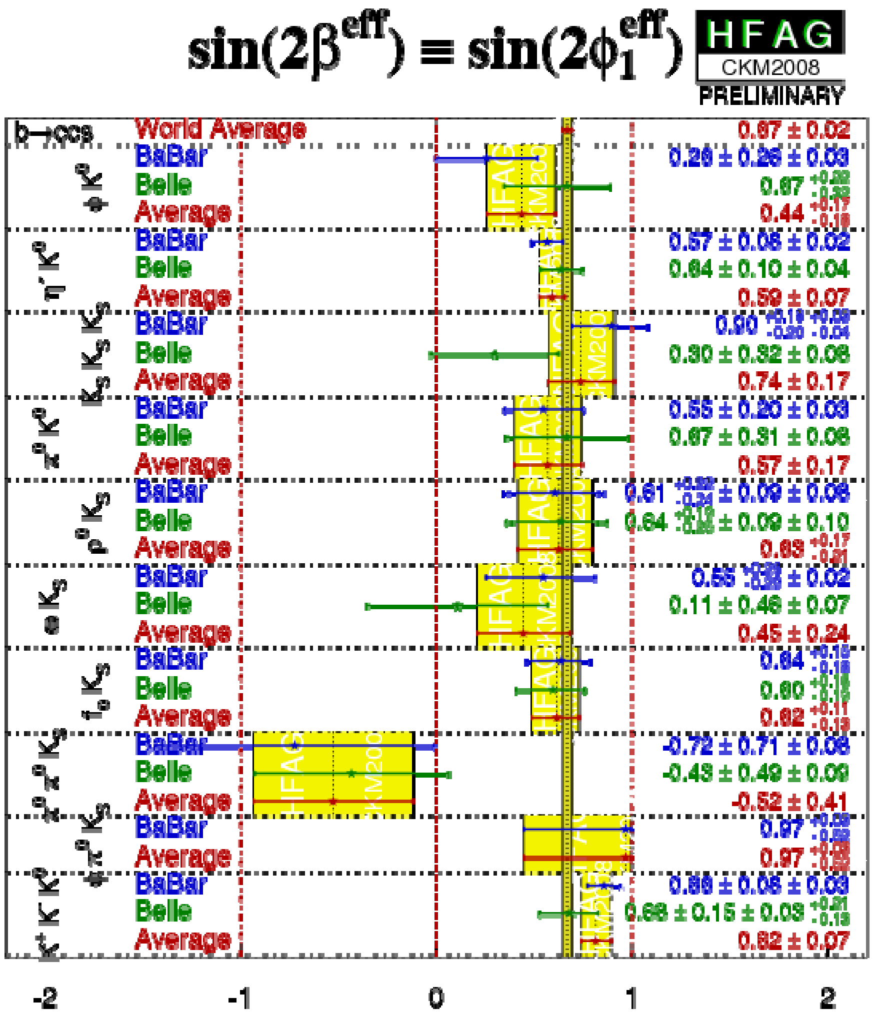

Details of Belle $K_S\pi^+\pi^-$ Analysis

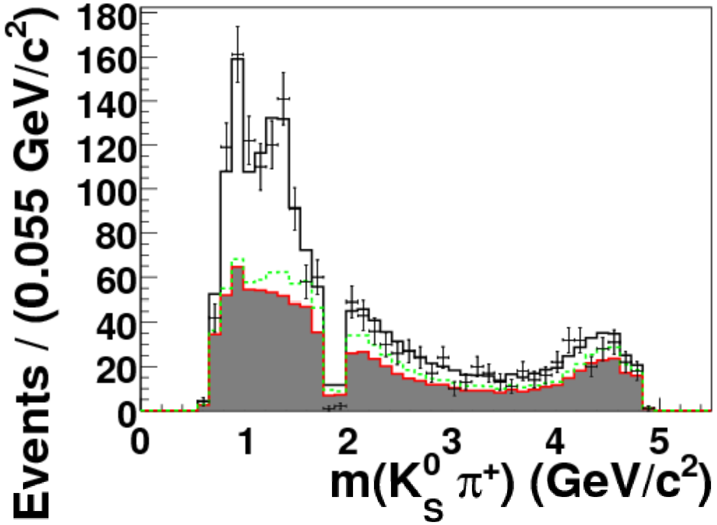

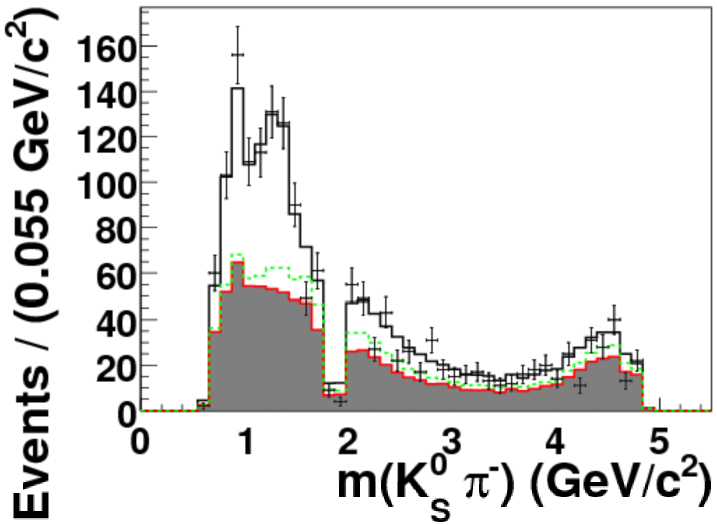

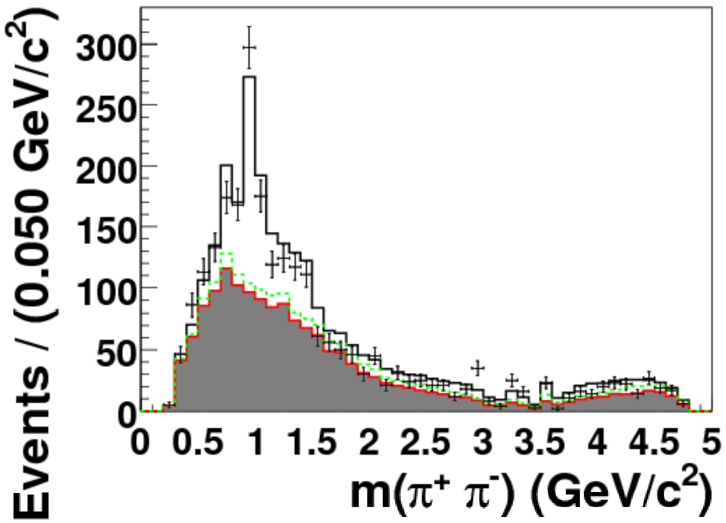

Details of Belle $K_S\pi^+\pi^-$ Analysis

Decay channel	Sol. 1 Fraction (%)	Sol. 2 Fraction (%)
$K^{*+}(892)\pi^-$	9.3 ± 0.8	9.0 ± 1.3
$K_0^{*+}(1430)\pi^-$	61.7 ± 10.4	17.4 ± 5.0
$\rho^0(770)K_S^0$	6.1 ± 1.5	8.5 ± 2.6
$f_0(980)K_S^0$	14.3 ± 2.7	14.9 ± 3.3
$f_2(1270)K_S^0$	2.6 ± 0.9	3.2 ± 1.2
$f_X(1300)K_S^0$	2.3 ± 0.8	6.0 ± 1.6
$(K_S^0\pi^+)_{\mathrm{NR}}\pi^-$	57.2 ± 11.4	55.9 ± 13.3
$(K_S^0\pi^-)_{\mathrm{NR}}\pi^+$	2.9 ± 4.7	6.4 ± 3.7
$(\pi^+\pi^-)_{\mathrm{NR}}K_S^0$	10.7 ± 3.5	7.7 ± 4.1
Total	167.1 ± 0.2	129.0 ± 0.2

Fit results of $K^+\pi^-\pi^0$ Analysis

isobar j	FF_j (%)	$\mathcal{B}_j$ (10^{-6})	A^j_{CP}
$K^{*+}(892)\pi^-$	$11.8^{+2.5}_{-1.5} \pm 0.6$	$4.2^{+0.9}_{-0.5} \pm 0.3$	$-0.19^{+0.20}_{-0.15} \pm 0.04$
$K^{*0}(892)\pi^0$	$6.7^{+1.3+0.7}_{-1.5-0.6}$	$2.4 \pm 0.5 \pm 0.3$	$-0.09^{+0.21}_{-0.24} \pm 0.09$
$(K\pi)^{*+}_0\pi^-$	$26.3^{+3.1+2.1}_{-3.8-2.0} \pm 4.9$	$9.4^{+1.1+1.4}_{-1.3-1.1} \pm 1.8$	$+0.17^{+0.11}_{-0.16} \pm 0.09 \pm 0.20$
$(K\pi)^{*0}_0\pi^0$	$24.3^{+3.0+3.7}_{-2.6-3.0} \pm 6.7$	$8.7^{+1.1+1.8}_{-0.9-1.3} \pm 2.2$	$-0.22 \pm 0.12^{+0.13}_{-0.11} \pm 0.27$
$\rho^-(770)K^+$	$22.5^{+2.2}_{-3.7} \pm 1.2$	$8.0^{+0.8}_{-1.3} \pm 0.6$	$+0.11^{+0.14}_{-0.15} \pm 0.07$
N.R.	$12.4 \pm 2.6^{+1.3}_{-1.2}$	$4.4 \pm 0.9 \pm 0.5$	$+0.23^{+0.19+0.11}_{-0.27-0.10}$
Total	$102.3^{+7.1}_{-4.0} \pm 4.1$	$35.7^{+2.6}_{-1.5} \pm 2.2$	$-0.030^{+0.045}_{-0.051} \pm 0.055$

Summary of $K^*\pi$ and ρK experimental measurements and theory predictions

	Branching Fraction (10^{-6})		A_{CP} (%)	
Mode	Exp.	QCDF	Exp.	QCDF
$K^{*0}\pi^+$	10.0 ± 0.8	8.9 ± 1.6	-2 ± 7	0.16 ± 0.16
$K^{*+}\pi^0$	6.9 ± 2.3	5.3 ± 0.8	4 ± 29	-41 ± 7
$K^{*+}\pi^-$	10.3 ± 1.1	9.1 ± 1.7	-25 ± 11	-48 ± 8
$K^{*0}\pi^0$	2.4 ± 0.7	3.9 ± 0.8	-15 ± 12	4.7 ± 1.1
ρ^+K^0	$8.0 \pm ^{1.5}_{1.4}$	10.3 ± 2.0	-12 ± 17	0.53 ± 0.21
ρ^0K^+	3.8 ± 0.5	4.8 ± 0.9	$42 \pm ^{8}_{10}$	46 ± 6
ρ^+K^-	$8.6 \pm ^{0.9}_{1.1}$	13.4 ± 2.3	15 ± 6	31.4 ± 4.6
ρ^0K^0	$5.4 \pm ^{0.9}_{1.0}$	7.5 ± 1.3	1 ± 20	-3.3 ± 1.3

Experimental numbers from HFAG Summer 2008, QCDF predictions from Chang et al., arXiv:0807.4295v3

Summary of $K^*\pi$ and ρK experimental measurements and theory predictions

- Agreement between experiment and theory is generally good
- Experimental precision on *CP* asymmetries much worse than theory errors
- Would be nice to have (updated) results from $K_S\pi^+\pi^0$ and $K^+\pi^0\pi^0$, particularly given large A_{CP} prediction in $K^{*+}\pi^0$
- Most results now coming from Dalitz-plot analyses
  - Additional information in the phases can be used to reduce the model dependence in extracting γ

The Square Dalitz Plot

$$m' \equiv \frac{1}{\pi}\arccos\left(2\frac{m_{K^+\pi^+} - m^{\min}_{K^+\pi^+}}{m^{\max}_{K^+\pi^+} - m^{\min}_{K^+\pi^+}} - 1\right),$$

$$\theta' \equiv \frac{1}{\pi}\theta_{K^+\pi^+},$$

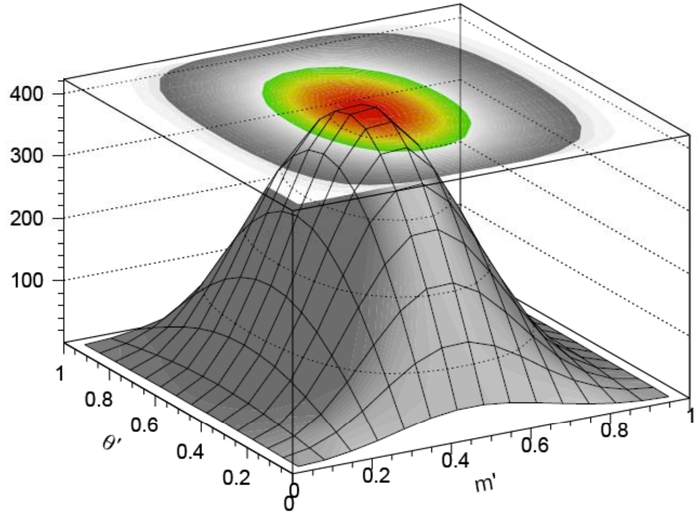

- Transformation of coordinates
- "Zooms" into the areas around the boundary of the conventional Dalitz plot
- Increases resolution in those areas of interest
- Used for all DP histograms in this analysis

LASS Lineshape

- The LASS parameterisation of the Kπ S-wave consists of the $K_0^{*0}(1430)$ resonance together with an effective-range nonresonant component:

$$\mathcal{M} = \frac{m_{K\pi}}{q\cot\delta_B - iq} + e^{2i\delta_B}\frac{m_0\Gamma_0\frac{m_0}{q_0}}{(m_0^2 - m_{K\pi}^2) - im_0\Gamma_0\frac{q}{m_{K\pi}}\frac{m_0}{q_0}},$$

$$\cot\delta_B = \frac{1}{aq} + \frac{1}{2}rq\,.$$

- We have used the following values for the scattering length and effective range parameters:

$$a = (2.07 \pm 0.10)\,(\mathrm{GeV}/c)^{-1}\,,$$

$$r = (3.32 \pm 0.34)\,(\mathrm{GeV}/c)^{-1}\,.$$

LASS Lineshape – plot

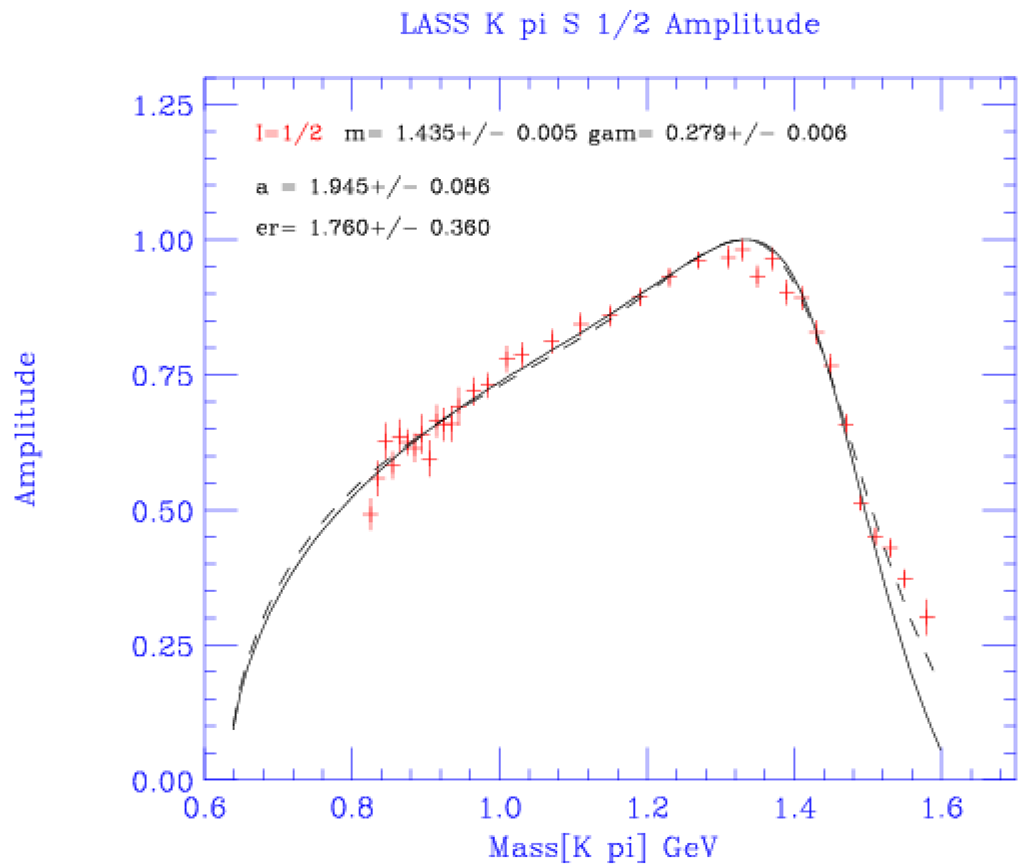

Flatté Lineshape

- Also known as a coupled-channel Breit–Wigner

$$R_j(m) = \frac{1}{(m_0^2 - m^2) - i m_0 (\Gamma_{\pi\pi}(m) + \Gamma_{KK}(m))}$$

- The decay widths in the $\pi\pi$ and KK systems are given by:

$$\begin{aligned}\Gamma_{\pi\pi}(m) &= g_\pi \left(\frac{1}{3}\sqrt{1 - 4m_{\pi^0}^2/m^2} + \frac{2}{3}\sqrt{1 - 4m_{\pi^\pm}^2/m^2} \right) , \\ \Gamma_{KK}(m) &= g_K \left(\frac{1}{2}\sqrt{1 - 4m_{K^\pm}^2/m^2} + \frac{1}{2}\sqrt{1 - 4m_{K^0}^2/m^2} \right) .\end{aligned}$$

- The fractional coefficients come from isospin conservation and g_π and g_K are coupling constants for which we assume the values obtained by the BES experiment:

$$\begin{aligned}g_\pi &= (0.165 \pm 0.010 \pm 0.015)\ \mathrm{GeV}/c^2 , \\ g_K &= (4.21 \pm 0.25 \pm 0.21) \times g_\pi .\end{aligned}$$

sPlots

[Nucl. Instrum. Meth. A 555 (2005) 356-369]

- The sPlots technique is a statistical tool that allows the distribution of a variable for a particular species, e.g. signal, to be reconstructed from the PDFs of other variables
- An sWeight is assigned to each event according to:

$$ {}_sW_n(y_e) = \frac{\sum_{j=1}^{N_S} \mathbf{V}_{nj} f_j(y_e)}{\sum_{k=1}^{N_S} N_k f_k(y_e)} $$

- Where NS is the number of species, V is the covariance matrix from the fit, f are the PDFs of the variables y, the subscript n refers to the species of interest and the subscript e refers to the event under consideration
- These sWeights have the property that:

$$ \sum_e {}_sW_n(y_e) = N_n $$

- A histogram in a variable (not in the set y) can then be filled with each event weighted by its sWeight
- This histogram will reproduce the e.g. signal distribution of that variable
- sWeights can also be used e.g. in order to correctly deal with signal reconstruction efficiency (ε) variation on an event-by-event basis
- In this case a branching fraction can be correctly determined from:

$$ BF = \sum_n \frac{{}_sW_n(y_e)}{\varepsilon_n N_{B\overline{B}}} $$